Current Status on the Manufacturing of Nanomaterials for Proton Exchange Membrane Energy Systems by Vapor-based Processes

Ryan J. Ouimet[1,2,], Thomas A. Ebaugh[1,2], Gholamreza Mirshekari[2], Stoyan Bliznakov[2], Leonard J. Bonville[2], Radenka Maric[1,2]*

1. Department of Chemical and Biomolecular Engineering, University of Connecticut, 191 Auditorium Road Unit 3222, Storrs, CT 06269

2. Center for Clean Energy Engineering, University of Connecticut, 44 Weaver Road Unit 5233, Storrs, CT 06269

KEYWORDS:

Atomic Layer Deposition; Chemical Vapor Deposition; Proton Exchange Membrane Fuel Cell; Proton Exchange Membrane Water Electrolysis; Reactive Spray Deposition Technology; Spray Pyrolysis.

ABSTRACT:

Development of novel technologies for catalyst synthesis and membrane electrode assembly (MEA) fabrication is of primary importance for further improvement of the performance and economics of proton exchange membrane fuel cells (PEMFCs) and proton exchange membrane water electrolyzers (PEMWEs). While the traditional manufacturing methods are time-consuming, energy intensive, and require many processing steps, the new vapor-based methods provide many benefits including the development of improved catalysts and catalyst supports, deposition of uniform thin films, reduction of catalyst loading, and minimizing the number of manufacturing steps. Recent publications in the field identified spray pyrolysis, reactive spray deposition technology, chemical vapor deposition, and atomic layer deposition as advanced vapor-based catalyst synthesis and deposition methods used for fabrication of MEAs for PEMFCs and PEMWEs. The MEAs fabricated via vapor-based processes have shown significant performance improvements in comparison to the state-of-the-art MEAs, which are attributed to better catalyst distribution, improved catalyst supports, and controlled, uniform catalyst layer microstructures. This review provides an overview of the vapor-based synthesis and deposition methods currently being used for the development of PEM-based devices. The advantages and disadvantages of these methods are critically compared and discussed while the outlook for future development is provided.

Introduction

As energy demand and greenhouse gas emissions are at historic highs, one of the many challenges scientists currently face is the development of clean and more efficient energy conversion devices that will decrease the amount of energy-related carbon emissions. One possible solution to reducing the energy-related greenhouse gas emissions is through the use of hydrogen as a clean energy carrier. Hydrogen is an attractive option for an energy carrier as it contains three times more energy per mass than gasoline[1]. While a significant percentage of hydrogen is currently produced from low-cost natural gas, diversifying the approaches available for affordable hydrogen production can enhance the long-term resilience of industries to price volatility[2]. For example, hydrogen gas production by water electrolysis uses renewable energy sources and results in the production of high-purity hydrogen which can be stored for extended periods without energy loss. When needed, the chemical energy of the hydrogen gas can then be converted to electrical energy with high efficiency using fuel cells. Conversion of the excess electrical energy to hydrogen via water electrolysis has been gaining tremendous interest in Europe and other parts of the world, because of the rapid penetration of the renewable energy sources into their energy sectors, which drives down the cost of the electricity. Hydrogen is an appealing storage medium for excess renewable energy because, once stored, it can be used in a variety of applications, including power generation, supplementation of the natural gas grid for increased efficiency, vehicle fueling, or as a high-value chemical feedstock for the green generation of fertilizer and other chemicals.The development of highly efficient, cost-effective, and durable fuel cells and electrolyzers is crucial to the implementation of a future hydrogen economy. Although these zero-carbon emission hydrogen-based clean energy conversion and storage devices have been a subject of increased

research and development interest during the past several decades, their performance, cost, and durability need further improvements to boost their commercialization. Today, cell stack manufacturing processes dominate the cost and energy use in PEM electrolyzer manufacturing. In particular, the acidic nature of the membrane limits the choices of catalyst materials to more expensive options such as platinum group metals (PGMs) and metal oxides.

Among the many different electrochemical systems currently under development, the proton exchange membrane fuel cell (PEMFC) and the proton exchange membrane water electrolyzer (PEMWE) are the most promising electrochemical energy conversion devices. In commercial development since the 1960s, PEMFCs have been shown to have many advantages compared to other fuel cell technologies. With high efficiency and low temperature operation, PEMFCs are able to satisfy performance and durability targets for many different applications such as portable devices and fuel cell electric vehicles[2–7]. Additionally, with hydrogen and oxygen as the only reactants, the PEMFC produces no greenhouse gases during operation and is a clean energy technology.

While PEMFCs convert the chemical energy of the hydrogen gas to electrical energy and produce zero emissions, it is equally essential to develop a clean hydrogen generator. According to the International Energy Agency, as of 2019, the global production of hydrogen is responsible for the emission of 830 Mt of CO_2 per year, as more than 99% of all dedicated hydrogen produced is the result of natural gas reforming or coal gasification[1]. One method that can significantly reduce the amount of greenhouse gases emitted from hydrogen production is through the use of water electrolysis, primarily when carbon-free sources such as solar or wind provide the power required for the electrolysis. PEMWEs operate by splitting water at the anode catalyst to produce oxygen gas and protons. The protons then travel across the proton exchange membrane (PEM) and react

at the cathode catalyst to form hydrogen gas. Some of the many benefits of PEMWEs are that they are durable with systems demonstrating over 50,000 hours of operation, the hydrogen produced has high purity, and they can operate at higher current densities than traditional alkaline electrolyzers, which allow for cost and size reductions[8].

While PEMFCs and PEMWEs are functionally different, they are structurally similar technologies. Both PEM devices consist of a number of cells assembled in a stack to obtain the desired power output for PEMFCs or the desired hydrogen output for PEMWEs. Each cell consists of membrane electrode assemblies (MEAs) between bipolar plates. The MEAs for both PEMFCs and PEMWEs consist of an anode gas diffusion layer/porous transport layer (GDL/PTL), anode catalyst layer, proton exchange membrane, cathode catalyst layer, and cathode GDL/PTL. Traditionally for a PEMFC MEA, both the cathode and anode catalyst layers consist of platinum or Pt alloy nanoparticles dispersed on a carbon catalyst support with a perfluorosulfonic acid (PFSA) ionomer to assist with the ionic transport and to extend the triple-phase boundary into the electrode. Traditionally for a PEMWE MEA, the cathode catalyst layer consists of platinum nanoparticles dispersed on a carbon catalyst support with a PFSA ionomer while the anode catalyst layer consists of iridium or iridium oxide nanoparticles with a PFSA ionomer to assist with the ionic transport. Catalytic materials are complex systems in which achieving the desired properties (i.e. activity, selectivity, and stability) depends on exploiting the many degrees of freedom in: surface and bulk composition, geometry, defects, interactions with the support material, control of the reacting environment, etc. Most importantly, the catalysts determine the performance of the cell and have a significant impact on the cost of the PEM device.

Despite the recent commercialization of these energy conversion devices, there is still no widespread use of PEMFCs and PEMWEs. The high cost of these electrochemical devices is one

of the main obstacles hindering their implementation. Even with high-volume manufacturing methods, the catalyst cost is projected to be the main contributor to the high cost of the MEAs. Available research indicates the best catalysts for PEM fuel cells and electrolyzers are expensive platinum group metal (PGM) nanoparticles[9,10]. While early PEMFCs are known to have used 4 mg_{Pt} cm^{-2}, advances since the 1980s have allowed for the reduction of catalyst loading to 0.4 mg_{Pt} cm^{-2} and projections trend lower[3]. Analysis coordinated by Whiston et al. in 2019 showed that 76% of experts rank the PGM catalyst cost as the primary barrier to reducing the cost for automotive PEMFCs[11]. A cost analysis performed by Wilson et al. in 2017 for 80 kW automotive PEMFCs showed that if the fabrication process were scaled to produce 500,000 systems per year, the catalyst layer would represent 41% of the PEMFC stack cost[12]. Similarly, for PEMWEs, following a significant reduction in bipolar plate costs, cost analysis shows that the catalyst and membrane account for 40% of the PEMWE cost[8].

Starting in the 1990s, two of the primary techniques for MEA fabrication include screen printing and decal transfer[3]. While effective, both technologies have challenges that need to be addressed in order to improve current MEA fabrication cost and scalability issues. Screen printing involves the application of a catalyst ink across a thin mesh screen onto the desired substrate. Screen printing is also a time-consuming and costly process due to the number of ink application and drying steps required to fabricate the catalyst layers[3,13]. The decal transfer method involves the application of a catalyst ink across a substrate, which is then transferred onto the desired membrane during a hot press step to attach the catalyst layer onto the membrane. While this step allows for a reduction in interfacial resistance between the catalyst layers and the membrane, the hot press step can lead to microstructural changes to the catalyst layer film and GDL/PTL while losing catalyst

materials to the internal portion of the GDL/PTL, which can lead to mass transport losses and decreased performance[3,14].

While ink-based deposition techniques have been important in MEA development to date, to reduce catalyst loadings and improve the economic viability of the PEM devices, further improvements are required. The novel MEA fabrication methods should support the deposition of catalyst layers with ultra-low catalyst loading, eliminate costly intermediate steps, and be scalable for commercial manufacturing. Among the many new processes under development, vapor-based catalyst synthesis and deposition methods have appeared as promising candidates for improving the economics of PEM devices while addressing many current manufacturing concerns. Through vapor-based processes, such as spray pyrolysis, chemical vapor deposition (CVD), and atomic layer deposition (ALD), catalyst thin films and nanoparticles can be developed with specific uniform growth rates. Therefore, they can be used for the deposition of highly active catalyst layers with ultra-low PGM loadings and desired thicknesses and porosity that will significantly improve the MEA's performance. Similarly, flame-based processes, such as flame spray pyrolysis and reactive spray deposition technology (RSDT), can synthesize catalyst nanoparticles and fabricate catalyst layers with ultra-low loadings while reducing the number of ink processing or drying steps. These processes will result in decreased manufacturing costs in addition to decreased catalyst costs.

This review examines recent progress in vapor-based nanoparticle synthesis and deposition methods, such as spray pyrolysis, RSDT, CVD, and ALD, for use in MEAs developed for advanced PEM-based devices. Each of the listed vapor-based processes are described in detail in individual sections that contain a brief overview of the vapor-based synthesis/deposition method, followed by a discussion of how the method works as well as some of the critical synthesis and/or

deposition parameters that impact the resulting catalyst nanoparticles or thin films. After describing the process and its advantages and disadvantages, a review of recently published literature is presented for the particular vapor-based method detailing how that method can be used for the fabrication of MEAs for PEMFCs and PEMWEs. Each of these major sections concludes with examples defining how each technology can be further improved for the fabrication of cost-effective MEAs with enhanced performance.

Spray Pyrolysis

Spray pyrolysis is a well-established method for catalyst synthesis that has been used since the 1980s as a process for fabrication of a variety of powders and films[15–17]. In 1993, Messing et al. published a review on spray pyrolysis for the production of ceramic powders that discusses its basic steps and fundamental mechanisms[18]. In 2005, the Cabot Corporation was assigned a patent for the production of electrocatalyst powders for energy devices by a spray conversion process[19]. This patent is particularly significant as it defines the fabrication of Pt/C catalysts by spray pyrolysis for use in PEM fuel cells. Recent literature has demonstrated the capability of spray pyrolysis to synthesize advanced catalysts and catalyst supports for PEM applications. These catalysts include metals (such as Pt), metal oxides (such as TiO_2), and non-PGM catalysts (such as $Co_xFe_{1-x}O_y$). Catalyst supports that have been produced by spray pyrolysis include metal oxides and various carbon supports[20–22].

Generally, spray pyrolysis involves the conversion of droplets of a liquid precursor mixture into a catalyst powder or film. To be truly considered spray pyrolysis (as opposed to spray drying), one or more of the precursors in these droplets must be thermally decomposed to create the product[15,18]. This normally occurs at temperatures greater than 300°C. The precursor mixture consists of one or more solvents and one or more precursors. Water is often used as the sole solvent[19–21,23–27], but

acids[28] and organic solvents[22] can be added. Some common precursors include metal chlorides[20,22,23,25–27], and metal nitrates[19,23,24]. Chloroplatinic acid is a common precursor for the synthesis of platinum nanoparticles[19,27,28]. Precursor mixtures can also contain templates, such as poly(methyl methacrylate) (PMMA) spheres[22], which form the microstructure of the product and are usually consumed during the spray pyrolysis process.

Spray pyrolysis is typically performed using three core components shown in Figure 1: (i) the atomizer (nebulizer), which generates droplets of the precursor solution, (ii) the reactor (pyrolytic chamber) or heated substrate, which thermally decomposes the precursor into the product particles, and (iii) the collection system, which collects the powdered product.

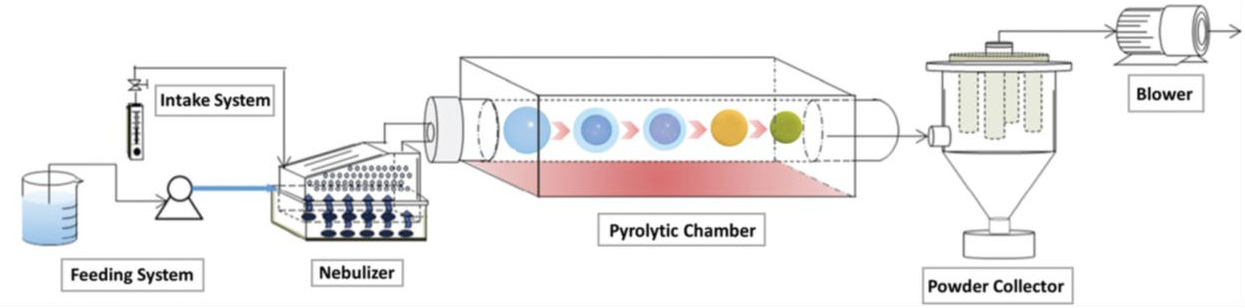

Figure 1. Graphical representation of the spray pyrolysis process. The precursor solution is fed to the atomizer (nebulizer), then to the reactor (pyrolytic chamber), and the product is collected in the collection system (powder collector). Reproduced from Leng et al. *Chem. Soc. Rev.* **2019**, *48* (11), 3015-3072. Copyright 2019 Royal Society of Chemistry.

Three types of atomizers are used in spray pyrolysis: ultrasonic, pneumatic (two-phase), and electrostatic[15]. Ultrasonic atomizers are most commonly used in laboratory settings because of their accessibility and ability to achieve relatively small droplets with a narrow size distribution at moderate production rates[15,29]. The ultrasonic atomizer works by using ultrasonic waves to excite the precursor mixture and produce droplets that can range from 1 micron to 100 microns in size[15]. Pneumatic atomizers are often used in commercial applications in order to achieve high production rates and accommodate precursor mixtures with high concentrations of suspended solids[15,19]. Pneumatic atomizers create droplets that can range from 10 microns to 100 microns and have

virtually no upper flow-rate limit[15]. The droplets produced by pneumatic atomizers have a relatively wide size distribution[29], which is a serious disadvantage for the fabrication of electrocatalysts. Alternatively, electrostatic atomizers create even smaller droplets than ultrasonic atomizers; however, their production rate is slow and they are not widely studied for the development of catalysts for application in PEM-based devices[15].

The droplets of precursor mixture that the atomizer produces are transported through the reactor or onto the heated substrate by a carrier gas. Various carrier gases can be used to achieve the desired product compositions. Air is used to obtain oxide nanoparticles[20,22,25,26]. Inert gas is used to obtain carbon-containing composites[21,23,24,27] and metal/metal-oxide composites[28]. Reducing gas is used to obtain metal nanoparticles[28]. The reactor or heated substrate supplies heat to the precursor droplets and carrier gas to evaporate the solvents, transform the precursor, and decompose any templates. At laboratory and commercial scales, tube furnaces are often used as the reactors[19–23,27,28,30]. A process can contain either one tube furnace or multiple tube furnaces in series to allow for flexibility in the process, such as introducing a new carrier gas between the furnaces[28]. For the fabrication of electrocatalysts for PEM-based devices, the tube furnaces are commonly operated at temperatures between 300°C and 800°C[19–23,27,28]. Additionally, instead of providing the thermal energy for the spray pyrolysis process from a tube furnace, heated substrates have also been used at the laboratory scale. Research by Kwong et al. examined the use of a heated titanium foil substrate at 200°C and 400°C for the fabrication of metal-oxide films[25,26].

It is generally accepted in the literature that particles fabricated by spray pyrolysis using a reactor (not a heated substrate) are formed by the "droplet-to-particle" method. By this method, one droplet of precursor solution renders one particle. These droplets can be the primary droplets originally formed by the atomizer, or smaller droplets that form through the fragmentation of the

primary droplets[28]. Figure 2 shows the many variations of the "droplet-to-particle" process for various precursor compositions and precipitation processes[18].

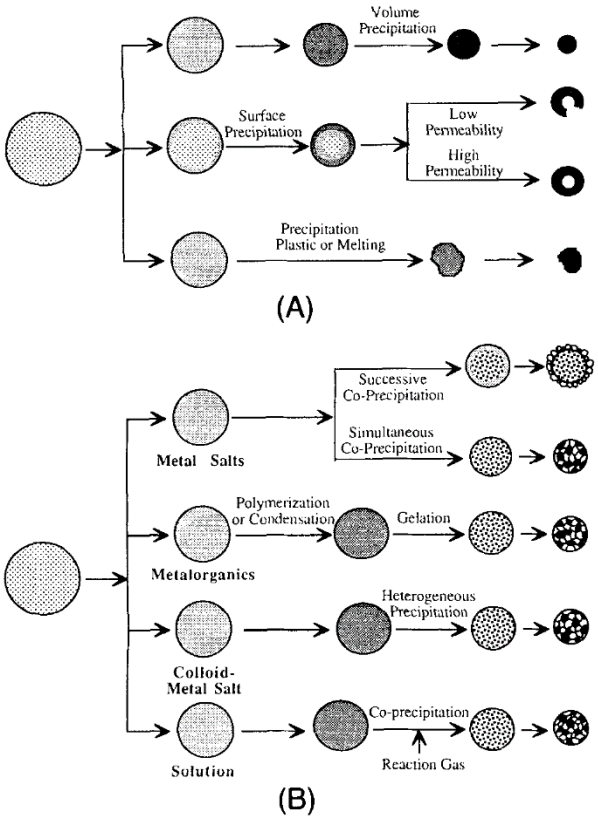

Figure 2. Flowcharts showing the effect of different precursor compositions and precipitation processes on (A) particle morphology and (B) the microstructure of composite particles. Reproduced from Messing et al. *J.Am. Ceram. Soc.* **1993**, *76* (11) 2707-2726. Copyright 1993 John Wiley & Sons, Inc.

In the droplet-to-particle mechanism, the chemistry of the solutes and solvents plays a critical role in determining the particle morphology as the interplay between solvent evaporation and solute diffusion impacts whether the particle is solid or hollow. When more than one precursor is used to form compounds, the relative solubilities, diffusivities, and decomposition temperatures of each precursor impact whether the particle adopts a core-shell structure[28].

When a heated substrate is used, the process by which the particles or film form on the substrate depends on the substrate temperature, droplet size, and volatility of the precursor solvent[16,17]. Various film formation processes and their resulting morphologies are shown in Figure 3.[17]

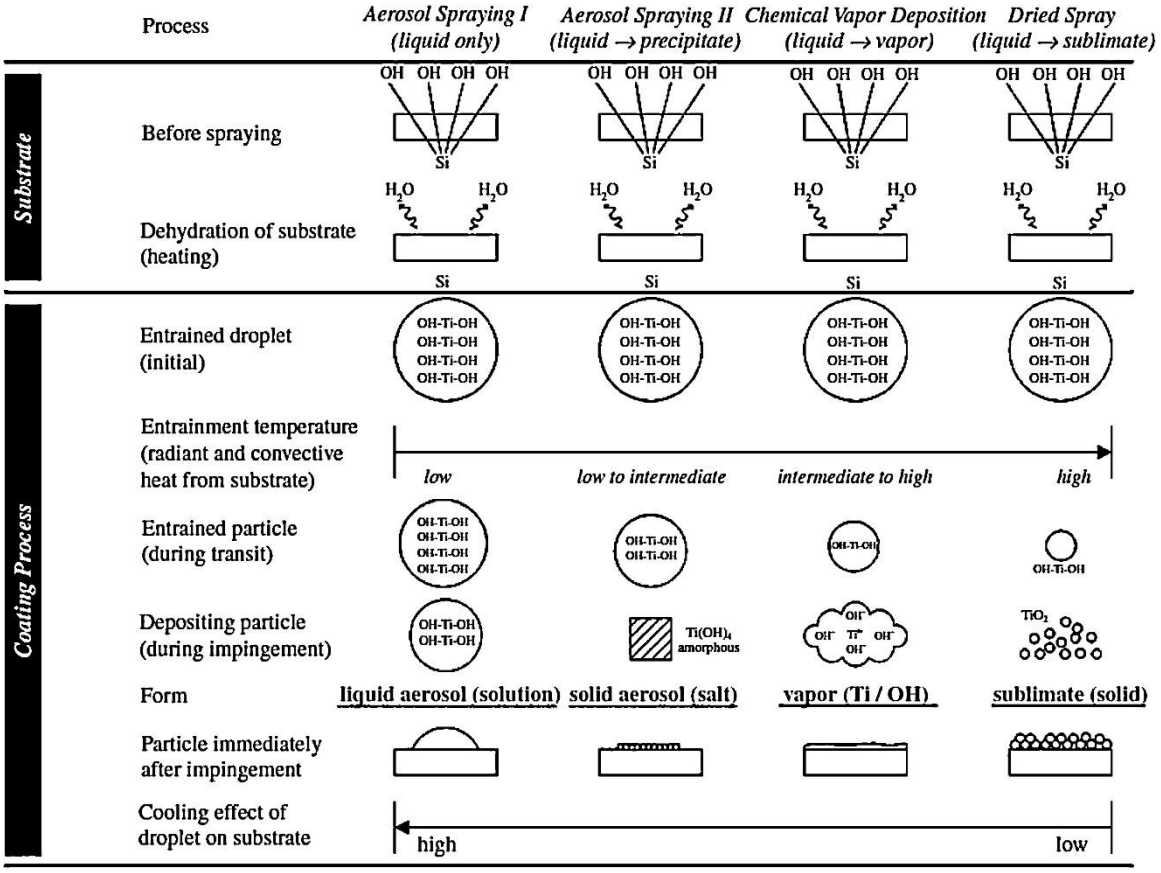

Figure 3. A diagram of the various processes of film formation during spray pyrolysis on a heated substrate. Reproduced from Guild et al. *Catal. Today* **2014**, *238*, 87-94. Copyright 2014 Elsevier

When a powdered product is not deposited onto a heated substrate, the particles must be collected by an additional apparatus. At the laboratory scale, these apparatuses include wash bottles[28], filters[20,23,27], and bubblers[21]. Wash bottles and bubblers are beneficial because they collect the particles in a liquid, which can prevent the product from agglomerating[31]. Particles collected in wash bottles or bubblers can be removed from the collection liquid by centrifugation and then be dried[28]. Particles can be separated from filters by ultrasonication in a solvent, followed by centrifugation and drying. Large-scale processes use cyclones[19] and electrostatic precipitators[30] to collect the products.

Advantages of Spray Pyrolysis

One of the most significant advantages is the control of the particle morphology over a range of length scales. Particle morphology and porosity are important not only for good catalytic performance, but also for the further processing of the catalyst powder into PEM devices[19]. As a result of the short reaction time associated with spray pyrolysis (ideally less than 10 seconds), the agglomeration of active species on the support material is limited, which helps achieve a good dispersion of active-species clusters between 0.5 nm and 10 nm in size[19]. Small, well-dispersed clusters of active material such as platinum are useful for increasing the mass-activity of the catalyst and reducing the overall cost. The short reaction time also allows the active-species particles to form metastable phases[15] such as particles with high-energy facets that have been shown to exhibit better catalytic performance in fuel cell applications than particles that contain thermodynamically stable phases[32,33].

In addition to improving the kinetic performance of the electrocatalyst, the morphology of the catalyst support particles needs to enable sufficient mass transfer of reactants to-and-from the catalyst active sites[19]. With spray pyrolysis, both the control of pore-size distribution of the support material (i.e., between 10 nm and 100 nm) and the specific surface area (i.e., up to 600 $m^2 g^{-1}$) of the catalyst can be achieved[19]. High porosity of the support material (i.e. >40%) is also important for reducing the density of the catalyst particles, which is beneficial when preparing a suspension of catalyst particles for further processing into components for PEM applications[19]. An additional benefit for the down-stream processing of catalyst particles fabricated by spray pyrolysis is that the particles (volume-average particle size between 1 micron and 100 microns) are spherical with a narrow size distribution. Spherical particles are easily processed and packed densely in the final-product film. The narrow particle size distribution is beneficial for avoiding nozzle clogging when depositing a slurry of dispersed particles[19].

Along with morphological control, spray pyrolysis offers tight control over the composition of the catalyst[15,19,25]. This is important for maintaining the oxidization state of active metallic species close to zero[19] and tailoring the composition of mixed-metal-oxides for PGM-free catalysts[25].

Aside from the benefits associated with the material fabricated by spray pyrolysis, the equipment and raw materials used for the process offer many inherent advantages as well. One distinct advantage of spray pyrolysis is its great flexibility as a result of using modular components[15]. For example, a patent by Cabot Corporation discusses the use of a spray dryer as a reaction chamber in place of a tube furnace for commercial-scale fabrication of Pt/C catalysts[19]. Using this configuration, the precursor reaches temperature up to 300°C, which is sufficient for the decomposition of the platinum precursor[19]. By processing the material at 300°C with the spray dryer, as opposed to the 700°C tube furnace, there is potential for cost reductions.

Applications of Spray Pyrolysis for PEMFCs

Many publications have used spray pyrolysis to fabricate catalysts for PEMFCs. Some processes fabricate the composite catalyst entirely by spray pyrolysis[27,28,34], while other processes fabricate the metal-oxide support with spray pyrolysis and later add the active species using wet methods[20]. Spray pyrolysis is also used to make a Zn-C precursor for the synthesis of N-doped carbon catalysts[24].

Košević et al. fabricated Pt/TiO_2 ORR/HER catalysts by spray pyrolysis using two different approaches, both using HCl as a solvent and N_2 and H_2 as carrier gases[28]. Nanoparticles fabricated using H_2PtCl_6 and tetra-n-butyl orthotitanate as platinum and TiO_2 precursors, respectively, exhibited insufficient platinum loading and are not an optimal catalyst for PEMFCs[28]. However, nanoparticles with 20 wt% platinum loading, fabricated at 650°C using H_2PtCl_6 as a platinum precursor with the TiO_2 support dispersed as a colloid in the precursor solution exhibited better

activity for the HOR/HER than platinum black in 1 M H_2SO_4 (pH≈0) at room temperature. A comparison of the cyclic voltammetry (CV) curves, measured at 50 mV s^{-1}, for the Pt/TiO_2 composite and platinum black is presented in Figure 4. The improved HOR/HER activity of the Pt/TiO_2 fabricated by spray pyrolysis is evident from the figure.

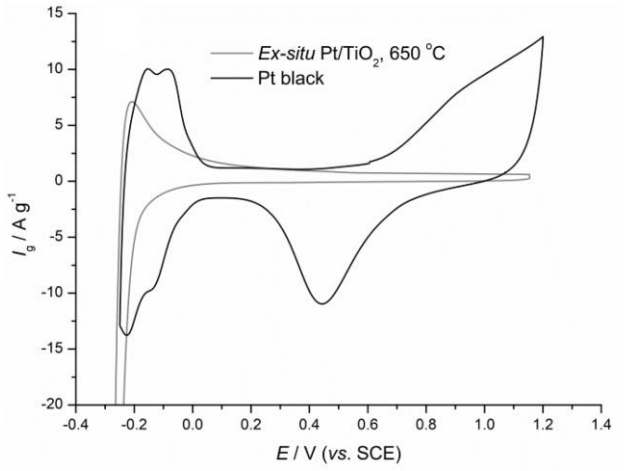

Figure 4: Cyclic voltammetry results with sweep rate of 50 mV s^{-1} for 20wt% Pt/TiO_2 and Pt black in 1M H_2SO_4 at room temperature. Reproduced from Košević et al. *Metals (Basel)* **2020**, *10* (11). Copyright 2020 MDPI

Pt-based catalysts have also been investigated by Kim et al. as ORR/OER catalysts in regenerative fuel cells[27]. Pt-Ir catalysts (1:1 mass ratio Pt:Ir) supported on reduced graphene oxide (rGO) were fabricated from an aqueous precursor mixture containing $IrCl_3$, H_2PtCl_6 and dispersed graphene oxide (GO). Argon was used as a carrier gas, and the particles were synthesized in a tube furnace at 600°C before being collected by a filter. Following the spray pyrolysis, the catalyst was heat treated in argon at 600°C to develop a crystalline structure[27]. Figure 5 presents a TEM image of the as-synthesized composite catalyst. The metal nanoparticles can be seen uniformly dispersed on the rGO sheet.

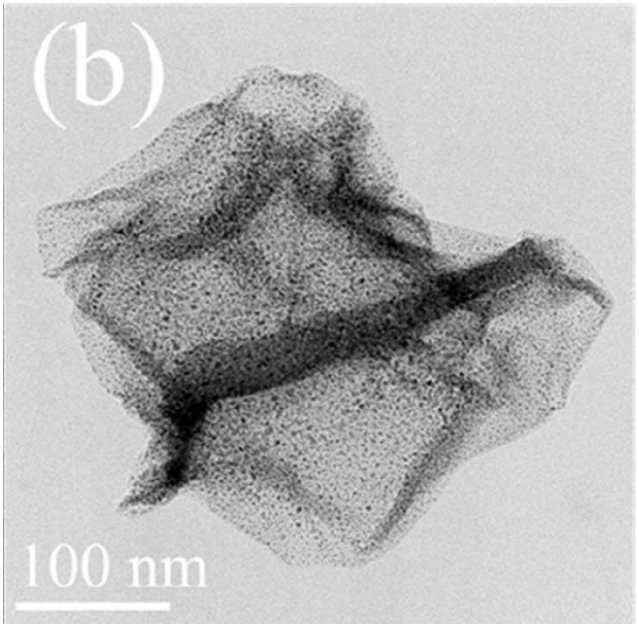

Figure 5. TEM micrograph of the as-synthesized Pt-Ir/rGO composite catalyst from Kim et al. Reproduced from Kim et al. *J. Power Sources* **2017**, *364*, 215-225. Copyright 2017 Elsevier

The durability of this composite catalyst was superior to that of commercially available Pt/C during potential cycling tests between 0.059 and 1.259 V (vs. RHE) at room temperature in nitrogen-saturated 0.1 M $HClO_4$. These tests were conducted for 4500 cycles using a RDE at 1600 rpm with a sweep rate of 50 mV s^{-1}. Figure 6 shows the loss in electrochemical surface area (ESA) of Pt/C and the as-synthesized catalyst during this testing.

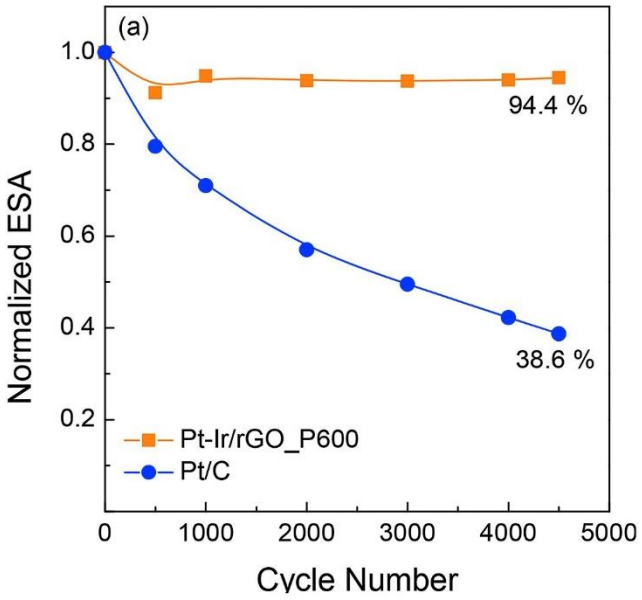

Figure 6. Electrochemical surface area (ESA) of the as-synthesized catalyst (Pt-Ir/rGO_P600) and Pt/C during cycling at 50 mV s-1 between 0.059 and 1.259 V (vs. RHE) at room temperature in nitrogen-saturated 0.1M $HClO_4$ using RDE at 1600 RPM. Reproduced from Kim et al. *J. Power Sources* **2017**, *364*, 215-225. Copyright 2017 Elsevier

Applications of Spray Pyrolysis for PEMWEs

Spray pyrolysis has also been used to develop catalysts or catalyst supports for PEMWEs[21–23,25–28]. Unsupported metal-oxide catalysts are deposited directly onto heated titanium foil[25,26]. Spray pyrolysis is also used to make a Zn-C precursor for the synthesis of N-doped carbon catalysts[24]. Böhm et al. developed a macroporous antimony-doped tin oxide (ATO) microparticle as a support for an IrO_2 OER catalyst[22]. Electron microscopy images of these particles and electrochemical test results are shown in Figures 7 and 8, respectively. The ATO particles were synthesized using tin (IV) chloride and antimony (III) acetate as precursors in ethanol and water. Poly(methyl methacrylate) beads with a mean diameter of 280nm were used as templates to develop the porosity in the ATO particles, which is evident in Figure 7. The precursor solution was atomized using an ultrasonic atomizer with air used as a carrier gas in a tube furnace set to 615°C. The IrO_2 was coated onto the ATO supports using a solvothermal method followed by thermal oxidization,

which achieved an even coating on the outside of the ATO particle and the surfaces of the pores.

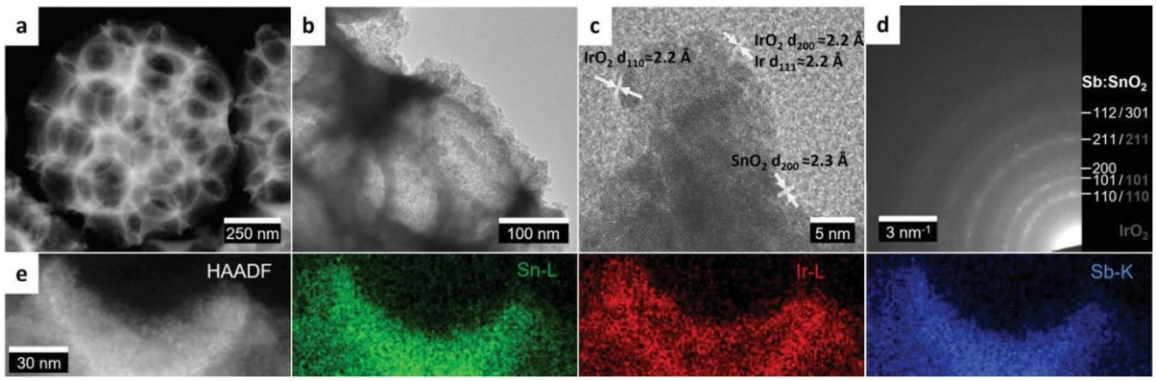

Figure 7. Transmission electron micrographs and EDX mapping of IrO_2 nanoparticles supported on microporous ATO microparticles templated with 280 nm PMMA beads. a-c) Electron micrographs, d) electron diffraction pattern, and e) STEM/EDX elemental mapping of an outer pore. Reproduced from Böhm et al. *Adv. Funct. Mater.* **2020**, *30*, 1906670. Copyright 2020 John Wiley & Sons, Inc.

As shown in Figure 8, Böhm et al. examined their IrO_2/ATO electrocatalyst using RDE and measured better oxygen evolution reaction (OER) activity than those achieved with the state-of-the-art IrO_2 on TiO_2.[22] The authors attributed the improved performance of this as-prepared OER catalyst to the morphology of the ATO support and to the homogenous distribution of the IrO_2 catalyst.

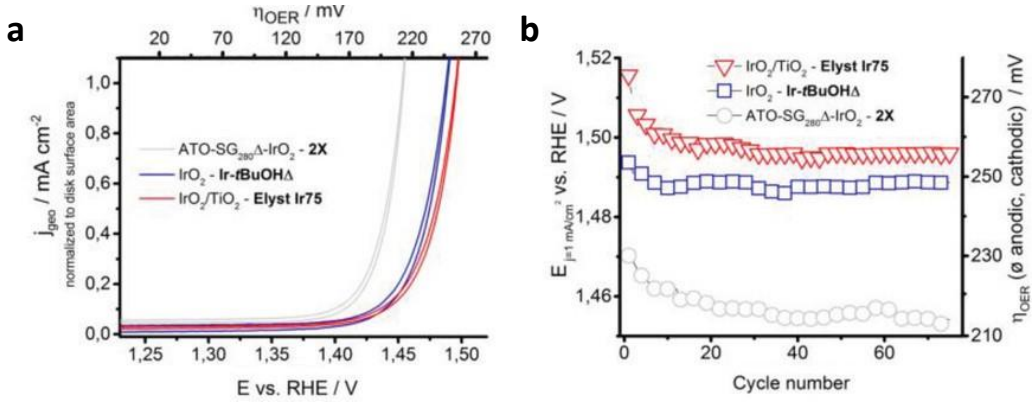

Figure 8. Electrochemical characterization of IrO_2 nanoparticles supported on microporous ATO microparticles at 60°C in 0.5M H_2SO_4. a) The 75th cycle of rotating disk electrode measurements of IrO_2 nanoparticles (blue), 25wt% Ir loaded ATO (grey), and commercial IrO_2/TiO_2 with 75wt% Ir loading (red). b) Overpotentials at 1 mA cm^{-2} for each RDE cycle. Reproduced from Böhm et al. *Adv. Funct. Mater.* **2020**, *30*, 1906670. Copyright 2020 John Wiley & Sons, Inc.

Work on non-PGM OER catalysts has also been done by Kwong et al., who investigated the fabrication of cobalt-doped hematite films[25]. Iron (III) chloride hexahydrate and cobalt (II) chloride hexahydrate were used as precursors in water. Air was used as a carrier gas to spray the precursor onto a titanium foil heated to 400°C. Various compositions of the catalyst with the general formula $Co_xFe_{1-x}O_y$ were fabricated. Figure 9 shows the activity and stability of the catalysts with different compositions.

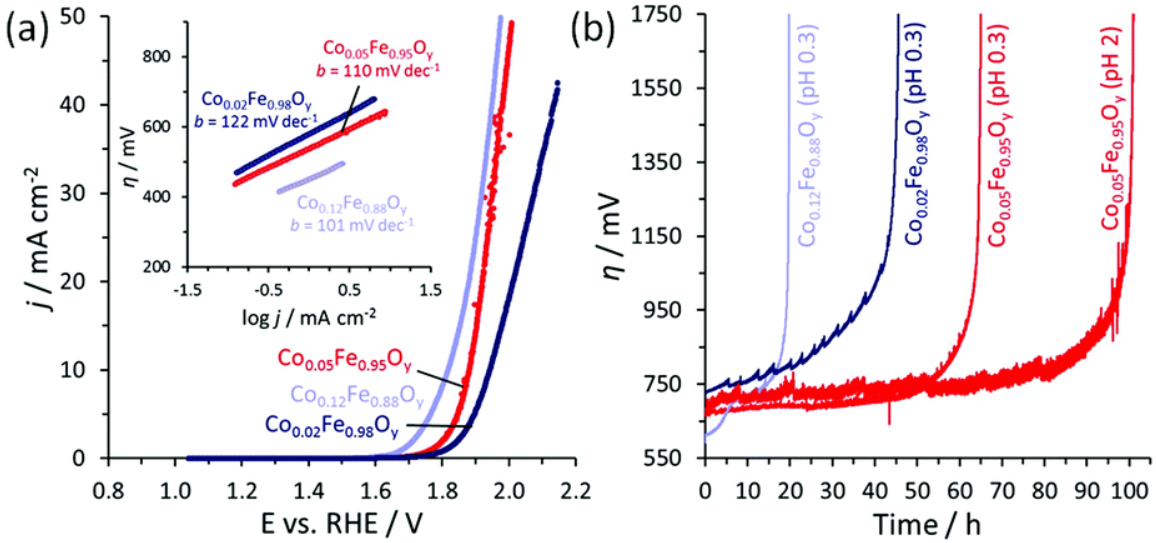

Figure 9. (a): Polarization curves and corresponding Tafel plots for various compositions of $Co_xFe_{1-x}O_y$. (b): Chronoamperometric measurements for various compositions of $Co_xFe_{1-x}O_y$ at j=10 mA cm^{-2} at pH 0.3 or pH 2. Reproduced from Kwong et al. *Chem. Commun.* **2019,** *55* (34), 5017-5020. Copyright 2019 Royal Society of Chemistry

The controlled doping of Co into the Fe_2O_3 lattice enhances the catalytic activity and improves electron transport throughout the catalyst. Figure 10 shows how the catalytic activity of $Co_{0.05}Fe_{0.95}O_y$ compares to that of FeO_y and IrO_y. While the IrO_y shows the best performance, the $Co_{0.05}Fe_{0.95}O_y$ offers the advantage of being PGM-free.

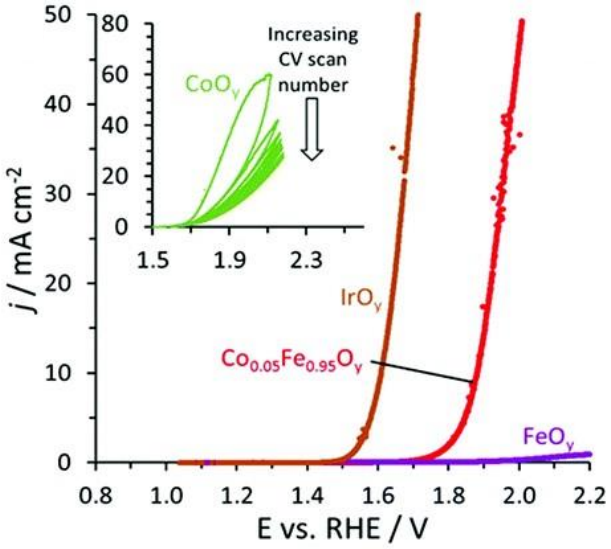

Figure 10. Polarization curves in 0.5M H_2SO_4 (pH=0.3) comparing $Co_{0.05}Fe_{0.95}O_y$, IrO_y, and FeO_y, catalysts. Inset: Cyclic voltammetry scans of CoO_y with subsequent cycling. Reproduced from Kwong et al. *Chem. Commun.* **2019,** *55* (34), 5017-5020. Copyright 2019 Royal Society of Chemistry

Future Development for Spray Pyrolysis

Despite the many advantages of spray pyrolysis, a notable shortcoming is a need for secondary processing of the catalyst material into PEM devices. This is particularly significant for industrial applications because additional processing steps lead to increased costs[33]. Therefore, one promising improvement for spray pyrolysis for PEM applications would be enabling the direct deposition of catalytic materials onto PEM components, such as PFSA membranes. However, using traditional spray pyrolysis conditions, direct deposition of the catalyst materials onto PFSA membranes would cause thermal degradation of the membranes. Therefore, in order to enable direct deposition of catalyst onto PFSA membranes, the gases and product particles would need to be cooled before reaching the PEM component. This could be achieved through the implementation of an air-quench, as it is done with RSDT as discussed below.

Future developments may also incorporate the sacrificial support method with the spray pyrolysis process to obtain catalysts with high surface area and unique morphologies. The

sacrificial support method develops materials with high surface area by first dissolving silica particles in a liquid solvent before adding precursor materials via wet impregnation methods. After the precursors adsorb to the silica, the particles are pyrolyzed to obtain the desired catalyst material before an etching process removes the silica to further increase the catalyst surface area. The sacrificial support method has also been used for the development of non-PGM catalysts with high activity due to condensed catalytic active sites[35,36]. While the sacrificial support method is not currently used with spray pyrolysis, the technical synthesis process steps are similar to where they may be incorporated into spray pyrolysis techniques to further improve the surface area of catalysts produced by spray pyrolysis.

Flame Spray Pyrolysis

Flame spray pyrolysis (FSP) is a specific type of spray pyrolysis, in which the energy needed for the evaporation of the solvent and decomposition of the precursor is provided by a flame instead of a heated substrate or tube furnace. According to Teoh et al., the precursor mixture provides at least 50% of the combustion enthalpy of the flame, as opposed to an external flame, such as a premixed oxy-hydrocarbon flame[37]. One distinct benefit of FSP is the elimination of the need for a heat-treatment step sometimes used in other spray pyrolysis processes; the high temperature of the flame leads to the direct formation of the desired crystal phases[15,33,37]. Carbon black and titanium dioxide are common industrial products produced by FSP, and they can readily be used as catalyst supports in PEM-based applications[33,37–40]. This proven capability at the industrial scale is promising for the low-cost mass-production of catalysts for PEMFCs and PEMWEs. FSP is also used for the development of metal-oxide and metal/metal-oxide catalysts for various application such as methane combustion, CO oxidation, and photocatalysts[39]. These metal/metal-oxide catalysts, such as Pt/TiO_2, could be used for PEM applications as demonstrated in Košević et al.[28].

Similarly, Ernst et al. have demonstrated that Pt/C catalysts fabricated by FSP are excellent candidates for other applications, such as the hydrogenation of cyclohexane[40]. Their one-step fabrication process simultaneously synthesizes the carbon support from xylene using one nozzle, and platinum nanoparticles from platinum acetylacetonate using an additional nozzle further downstream. A diagram of the process is shown in Figure 11.

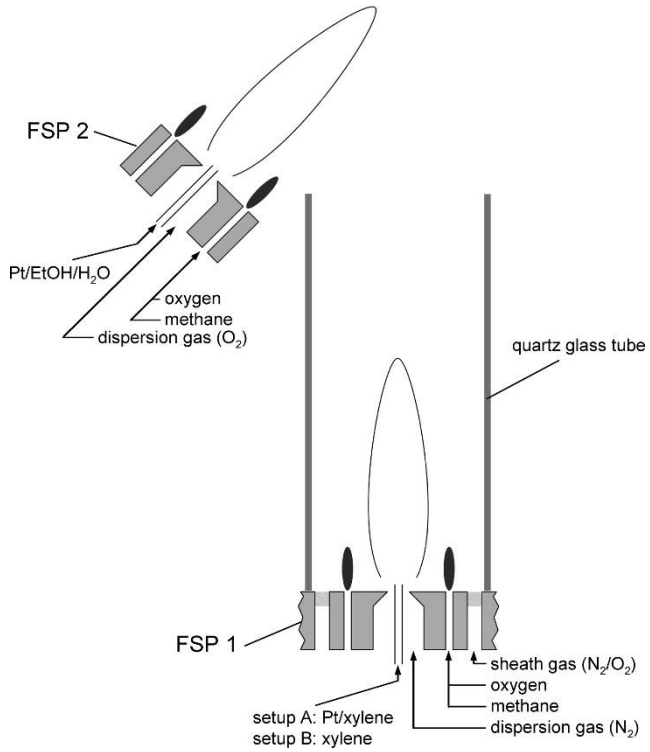

Figure 11. Diagram of the flame spray pyrolysis process used by Ernst et al. for the fabrication of Pt/C catalysts. To fabricate Pt nanoparticles dispersed on a carbon support, FSP 1 is fed with xylene to synthesize the carbon. Further downstream, the platinum is then sprayed from FSP 2 using platinum acetylacetonate as a precursor in ethanol and water. Reproduced from Ernst et al. *Chem. Mater.* **2008**, *20* (6), 2117-2123. Copyright 2008 ACS Publications

While catalysts synthesized by FSP have shown high performance for a wide variety of applications, FSP has also received attention for the fabrication of catalysts and catalyst supports specifically for application in PEM-based devices. For example, Dahl et al. used flame spray pyrolysis to fabricate metal-doped titanium oxide and tin oxide powders as supports for cathode catalysts for PEM fuel cells[41]. In another publication, Dahl et al. fabricated a Pt catalyst supported on antimony- and niobium-doped tin oxide supports, which have better corrosion resistance than

traditional carbon supports used in PEMFCs[42]. To produce these materials with FSP, tin (II) 2-ethylhexanoate, antimony (III) ethoxide, niobium (V) ethoxide, and platinum (II) acetylacetonate were used as precursors dissolved in p-xylene and acetone[42]. As-fabricated catalysts have notably higher specific surface area and better electronic conductivity than the commercial standard.

Reactive Spray Deposition Technology

Reactive Spray Deposition Technology (RSDT) is an advanced flame-based catalyst synthesis and deposition process that has been developed for one-step fabrication of MEAs for PEM-based electrochemical devices. While this process is similar to flame spray pyrolysis with respect to nanoparticle formation in a flame, RSDT has a major advantage since it allows for the direct deposition of the nanomaterials onto the desired substrates. Researchers have used RSDT as a cost-effective method for the fabrication of MEAs for both PEMFCs[43–48] and PEMWEs[49–51]. By significantly reducing PGM catalyst loadings, developing non-PGM catalysts, and eliminating costly manufacturing processing steps, the RSDT process is a method that has the ability to fabricate advanced MEAs for application in economically viable fuel cells and electrolyzers.

To fabricate nanomaterials by RSDT, a precursor solution containing the desired elemental composition of the final catalyst is prepared. The precursor solution mixture is chosen by first determining an appropriate organometallic precursor compound and solvent combination[52,53]. The precursor must be able to completely dissolve in the solvent such that there is no precipitation of precursor materials in order to avoid an inaccurate stoichiometry of the catalyst or inconsistent deposition results. Additionally, the solvents must be chosen such that the heat provided by the solvent combustion in the RSDT process will allow for the decomposition of the precursor materials. Once the precursor solution is prepared and filled into the RSDT pumps, the solution

passes through a heated line before passing through a small orifice needle. The increased pressure and temperature of the solution results in the formation of an atomized mist as it passes through the needle. The resulting aerosol is then ignited to create the RSDT flame, as shown in Figure 12. This flame is stabilized using a methane/oxygen pilot mix, while the combustion of the solvents is controlled with the addition of oxygen flowed to the needle tip. The resulting RSDT flame promotes the combustion of the solvent, which then provides the heat necessary to decompose the precursor materials to the desired catalyst material. As-synthesized catalyst nanoparticles then directly collide with the desired substrate which is moved over a specified spray area in the direct path of the RSDT flame to develop a uniform catalyst layer.

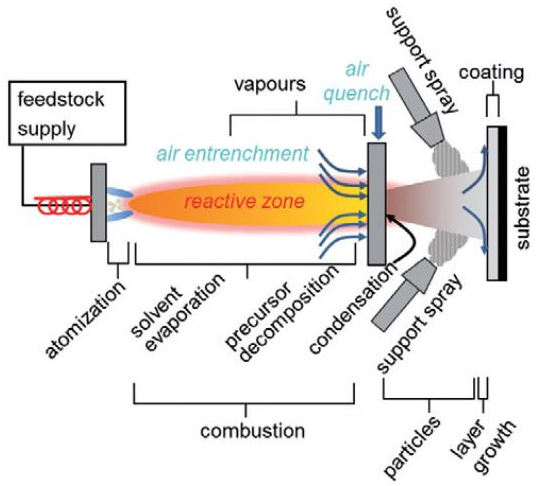

Figure 12. Schematic representation of reactive spray deposition technology (RSDT). Reproduced from Maric *Fuel Cells Bull.* **2012**, *2012* (4), 15. Copyright 2012 Elsevier

In addition to the RSDT flame, other components, such as an air quench or secondary spray nozzles, can be added to the RSDT process to significantly affect the development of the nanoparticles and resulting thin film microstructures. These components allow for the RSDT process to have many advantages as they ensure precise control of the properties of the deposited catalysts. One important component for the RSDT fabrication of nanoparticle catalysts for advanced MEAs is the incorporation of an air quench[52]. By positioning a flow of air in the flame

path, the air quench extinguishes the flame at a specific distance from the needle tip. With catalyst particle size increasing as the particle passes through the flame, particle growth can be controlled by the placement of the air quench. In addition to controlling particle size, the air quench also reduces substrate and catalyst temperatures to allow for the direct deposition on a variety of substrates, including perfluorosulfonic acid (PFSA) membranes. As a result of the reduced temperatures of the substrate, the RSDT process can directly deposit catalyst layers onto PEM membranes, which enables the direct one-step MEA fabrication process. In addition to the use of the air quench, secondary spray nozzles can be placed after the quench, as shown in Figure 12, to allow for the deposition of catalyst support materials. Rather than using multiple catalyst ink application and drying steps for MEA fabrication, a slurry containing both the catalyst support and ionomer components of a PEM catalyst layer can be sprayed through the RSDT secondary nozzles[47,48]. With this setup, the catalyst nanoparticles produced through the RSDT flame collide with the support material and ionomer prior to reaching the substrate to create complete catalyst layers in one step.

Advantages of RSDT

With many process parameters and additional components that can be used with the base RSDT flame, the RSDT process allows for flexibility in the catalysts being deposited. Research by Roller et al. examined how variations in the RSDT deposition parameters result in changes in particle size[52,53]. While examining the deposition of Pt nanoparticles with RSDT, Roller et al. demonstrated that varying the tip oxygen gas flow rate from 5.8 SLPM to 9.3 SLPM increased the mean Pt particle size diameter from 2.2 nm to 6.9 nm. The TEM micrographs and the estimated particle size distributions of as-fabricated Pt nanoparticles are presented in Figure 13.[52] Additionally, they determined that propane content in the precursor solution also has an impact on the particle size.

The authors reported that a solution with 10 wt% propane is capable of depositing 3.6 nm Pt particles while a solution with 20 wt% propane is capable of depositing 6.8 nm particles[52]. As a result, the RSDT process provides the ability to define the deposition parameters that will generate nanoparticles of specific sizes, which can be selected depending on the desired application.

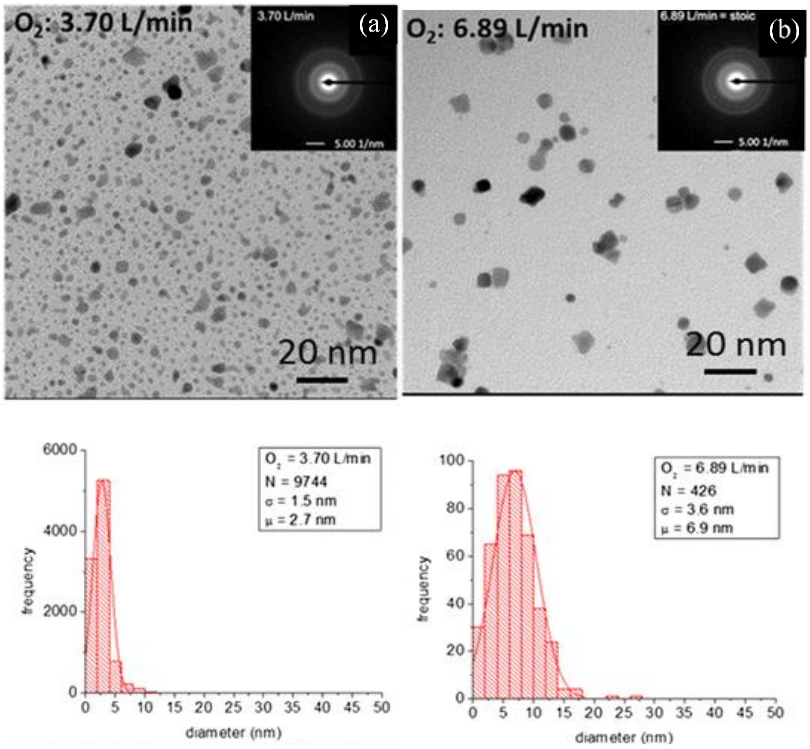

Figure 13. TEM micrographs and particle size distributions of Pt nanoparticles fabricated by RSDT when flowing tip oxygen at (a) 3.70 L min^{-1} and (b) 6.89 L min^{-1}. Reproduced from Roller et al. *J. Mater. Sci.* **2017**, *52* (16), 9391-9409. Copyright 2017 Springer

Furthermore, the RSDT process is capable of depositing a wide range of supported and unsupported catalysts with various ionomer contents. The RSDT process has been used to examine the effect of different carbon supports on the catalyst's performance by using Ketjen Black EC600JD[43,44,47,48], Vulcan XC72-R[45,49–51,54], multiwalled carbon nanotubes (MWCNTs)[47,48], and other graphitized carbons[47]. By simply modifying the carbon/ionomer slurry, it is possible to use the RSDT method to understand the effect of carbon supports, ionomers, or the ionomer content on MEA performance.

Applications of RSDT for PEMFCs

The RSDT method has been used for the fabrication of large MEAs for economically viable advanced PEMFCs. It has been recently reported that RSDT-fabricated MEAs with ultra-low PGM loadings have demonstrated excellent activity and durability comparable to state-of-the-art commercial MEAs that have 2-3 times higher PGM loadings in their catalyst electrodes. Yu et al. used RSDT to deposit PEMFC electrodes with Pt loadings of 0.1 mg_{Pt} cm^{-2} and 0.05 mg_{Pt} cm^{-2} for the cathode and the anode, respectively[47]. To confirm the uniform distribution of the platinum nanoparticles on the carbon supports, catalyst samples were examined by TEM. The TEM micrographs shown in Figure 14 demonstrate the uniformity of the Pt nanoparticles on the carbon supports following the RSDT process. During MEA testing at 0.9 V, 80°C, 280 kPa_{abs}, and 100% relative humidity, the estimated mass activity of the Pt/KB catalyst is 0.51 A mg_{Pt}^{-1}, which exceeds the 2020 DOE target of 0.44 A mg_{Pt}^{-1}.

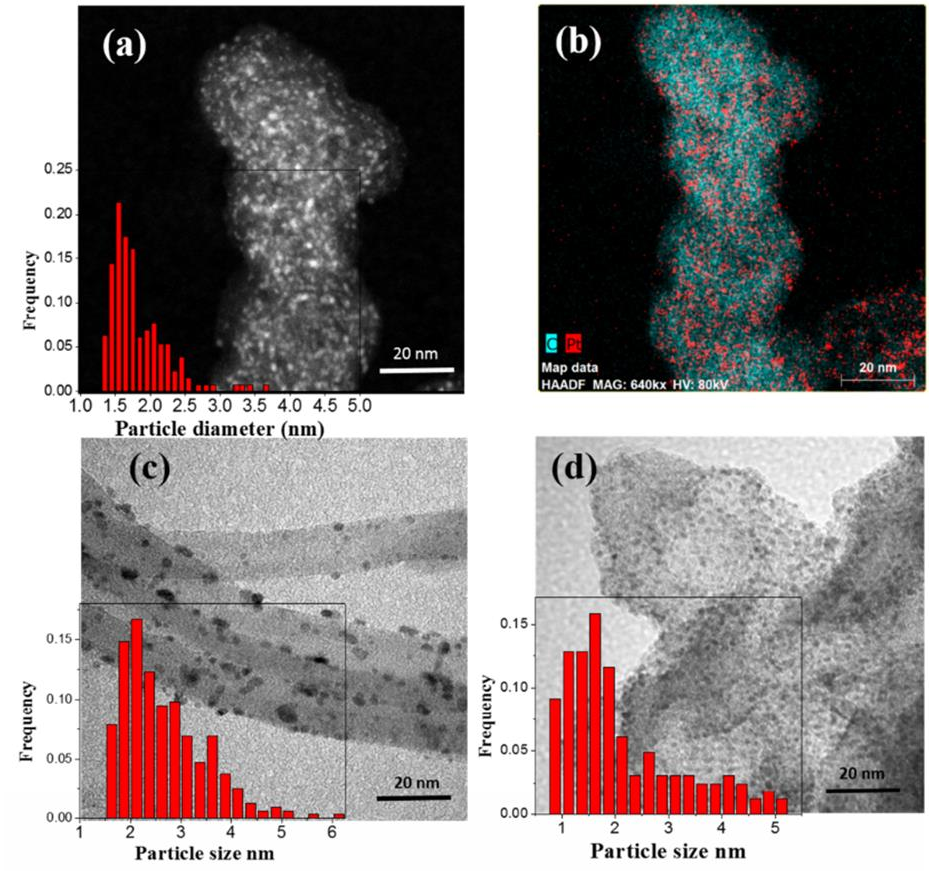

Figure 14: (a) High angle annular dark field (HAADF) image and (b) EDX elemental mapping of Pt and C (b) for Pt supported on Ketjen Black. (c) Bright field TEM image of Pt/MWCNT and (d) Pt/rGO. Pt particle size distributions are noted in the figure inserts. Reproduced from Yu et al. *ECS Trans.* **2015**, *69*, 487-496. Copyright 2017 IOP Publishing

In an effort to reduce cell degradation as a result of Pt depletion in the fuel cell cathode, the RSDT has also been used to fabricate cathode catalyst layers with gradient distribution in both Pt particle size[43] and Pt loading[44]. Yu et al. fabricated these gradient catalyst layers by adjusting either solution/slurry flow rates or other deposition parameters, which dictated the particle size. In order to obtain a gradient distribution in the Pt nanoparticles size from 2 nm to 5 nm, the solution flow rate, gas flow rates, as well as the quench position and flow rate were all[43]. The Tafel plots of MEAs fabricated with cathodes with gradient distribution of either Pt particle size (Type I) or Pt loading (Type II) are measured in H_2/Air and H_2/O_2 atmosphere and are compared in Figure 15. The authors concluded that the Type II MEAs have improved end-of-test performance in

comparison to the control MEAs with a uniform 2 nm Pt particle size and uniform loading in their cathodes, as well as to the Type I MEAs.

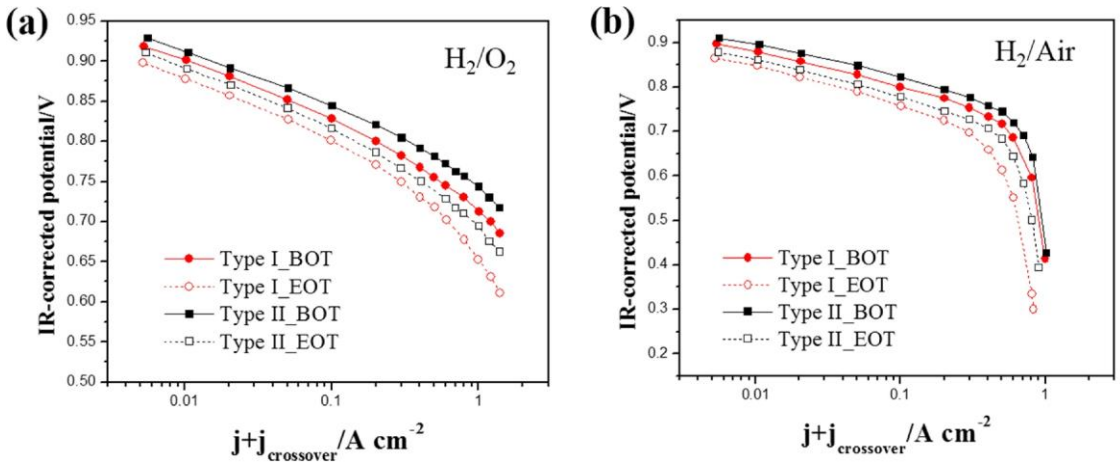

Figure 15. Tafel plots comparing Type I (gradient Pt particle size) and Type II (gradient Pt loading) MEAs at both the beginning-of-test (BOT) and end-of-test (EOT) under (a) H_2/O_2 conditions and (b) H_2/Air conditions. Reproduced from Yu et al. *Electrochim. Acta* **2017**, *247*, 1169-1179. Copyright 2017 Elsevier

Additionally, the RSDT process has been used to develop novel PGM and non-PGM catalysts to aid in the reduction of fuel cell capital costs. Fabrication of core-shell electrocatalysts for PEMFCs is one example that demonstrates the ability of the RSDT process to substantially reduce the PGM catalyst content loadings in the MEA electrodes. Roller et al. have demonstrated the ability to develop core-shell catalysts using the RSDT process by developing Pd-Ru and Pd@Pt catalysts[54].

Applications of RSDT for PEMWEs

While significant research has been performed on RSDT with PEMFC applications in mind, similar research needs to be performed to improve the economic viability of PEMWEs. These electrochemical energy conversion devices require even higher PGM loadings in their catalyst layers to operate at current densities of practical interest. Thus, one major challenge for PEMWEs is the cost associated with the PGM loading in the catalyst layers. Currently, the state-of-the-art commercial PEMWEs use iridium oxide anode catalysts and platinum nanoparticle cathode

catalysts with the typical loadings of 1-3 mg_{PGM} cm^{-2} in each electrode[55–57]. As seen with the PEMFC research, RSDT can fabricate catalyst layers with significantly lower PGM loadings. According to Yu et al., the RSDT process is capable of fabricating PEMWE anodes with IrO_x loading of 0.08 mg cm^{-2} and cathodes with Pt loading of 0.3 mg cm^{-2}.[49] As shown in Figure 16, despite an order of magnitude reduction in the PGM loadings on both electrodes in comparison to the commercial MEAs, the RSDT-fabricated MEA showed better performance. This RSDT-fabricated MEA demonstrated long-term stability for over 4500 hours of operation at steady-state conditions with a degradation rate of 36.5 µV hr^{-1} at the beginning of the test and 11.5 µV hr^{-1} near the end of the test.

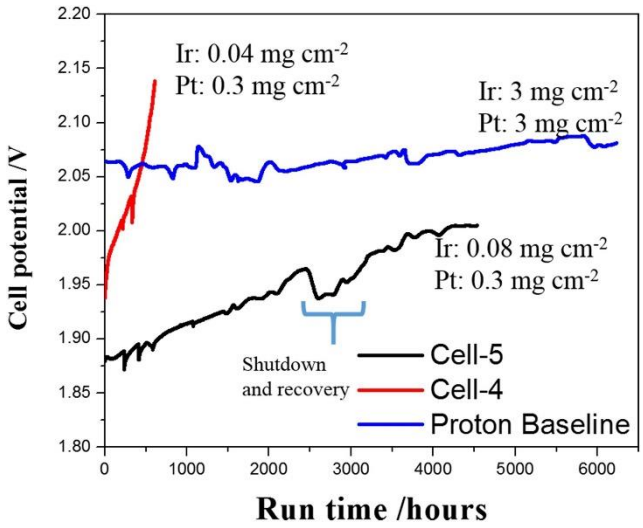

Figure 16. Long-term durability results of PEMWEs developed by RSDT compared to a commercial baseline PEMWE. Reproduced from Yu et al. *Appl. Catal. B Environ.* **2018**, *239* (July), 133-146. Copyright 2018 Elsevier

The RSDT process is a unique methodology not only for the fabrication of catalyst layers with ultra-low PGM loadings for advanced MEAs, but also for the deposition of recombination layers (RLs) that can reduce the hydrogen crossover in PEMWEs. Recent publications have shown that the integration of a Pt RL within the membrane of the PEMWE MEAs ensures the effective recombination of the hydrogen and oxygen molecules into water, and thus substantially reduces the H_2 crossover in the PEMWE stack[58–60]. With a lower flammability limit (LFL) of 4% hydrogen

in oxygen, typical PEMWEs need to be operated at conditions such that safety is maintained at all times. Most of the commercial PEMWEs have an integrated safety system that will shut down the PEMWE if there is more than 2% hydrogen in oxygen outlet stream. By incorporating the recombination layer in the PEMWE, H_2 crossover can be reduced to ensure the safe operation of the PEMWE system, and performance can be improved. Recent studies have shown that the RSDT-fabricated Pt RLs within the volume of the Nafion® membranes effectively reduced H_2 crossover in the MEAs. Ouimet et al. used the RSDT method to deposit a thin Pt film on a Nafion® N117 membrane that was then laminated by putting a Nafion® N211 membrane on top of the RL, and then hot pressed together[61]. As shown in Figure 17, a MEA without an RL exhibited H_2 crossover that ranged from 30-50% of the LFL during steady-state operation at current densities of 0.58, 1.16, and 1.86 A cm^{-2}. However, the H_2 crossover has been reduced to less than 10% of the LFL at all operating conditions for the MEAs containing an RSDT-fabricated RL.

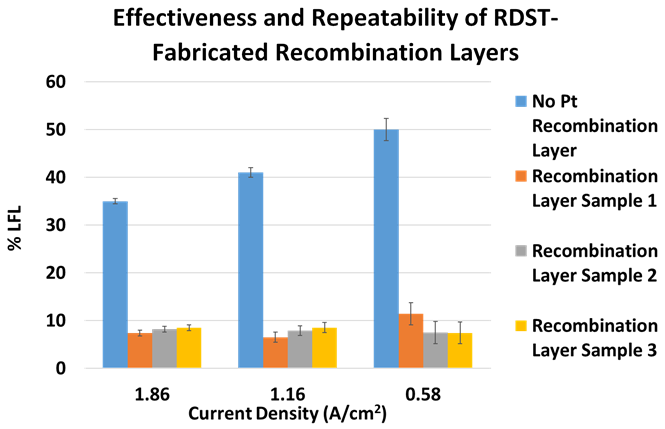

Figure 17. Hydrogen crossover of MEAs with and without RSDT-fabricated Pt recombination layers at various current densities.[61]

Future Development Strategies for RSDT

Despite encouraging PEMFC and PEMWE performance from MEAs developed by RSDT, there are opportunities to improve upon the deposition efficiency and scalability of electrodes

manufactured by the RSDT process. To date, the RSDT process has been utilized for developing cells with an active area of 25 cm^2, 45 cm^2, or 86 cm^2. Additional research has been performed to scaleup the active area of the cells to 711 cm^2. In order for the RSDT process to become a more complete commercial manufacturing technique, the RSDT process needs to be modified from a lab-scale method to a large-scale industrial technology to allow for rapid MEA manufacturing.

The RSDT process can also further reduce the dependency on PGM catalysts for PEM systems by developing non-PGM materials. The research conducted by Poozhikunnath et al. showed that the RSDT process can be used for the synthesis of non-PGM catalysts for alkaline exchange membrane fuel cells (AEMFCs)[62]. Utilizing similar processes, the RSDT process could further be used for the development of materials that could be utilized for PEM-based applications, further reducing the need for PGM catalysts.

Chemical Vapor Deposition

Chemical vapor deposition (CVD) is a generic name for a group of complex synthesis processes that involve depositing thin coatings on a substrate surface in which the chemical gaseous components react close to or on the hot substrate. The CVD process has emerged as a useful manufacturing technique for producing materials with high purity, density, and strength in industrial sectors such as the ceramic and semiconductor industries[63].

In the CVD process, the substrate is usually activated by heating, radiation, or plasma to produce a solid deposit. Figure 18 details a schematic of a typical CVD reactor[64]. In a typical CVD system, reactant gases, also called precursor gases, are delivered into a reaction chamber at a certain temperature. The inlet gases pass through the chamber, come into contact with the hot substrate, and react to form and deposit the target materials onto the surface of the substrate. An inert gas,

such as Ar, is usually utilized as a diluent gas. The critical parameters which affect the properties of the fabricated materials are the composition of the reaction gas mixture, substrate temperature, and gas flow pressure[65,66].

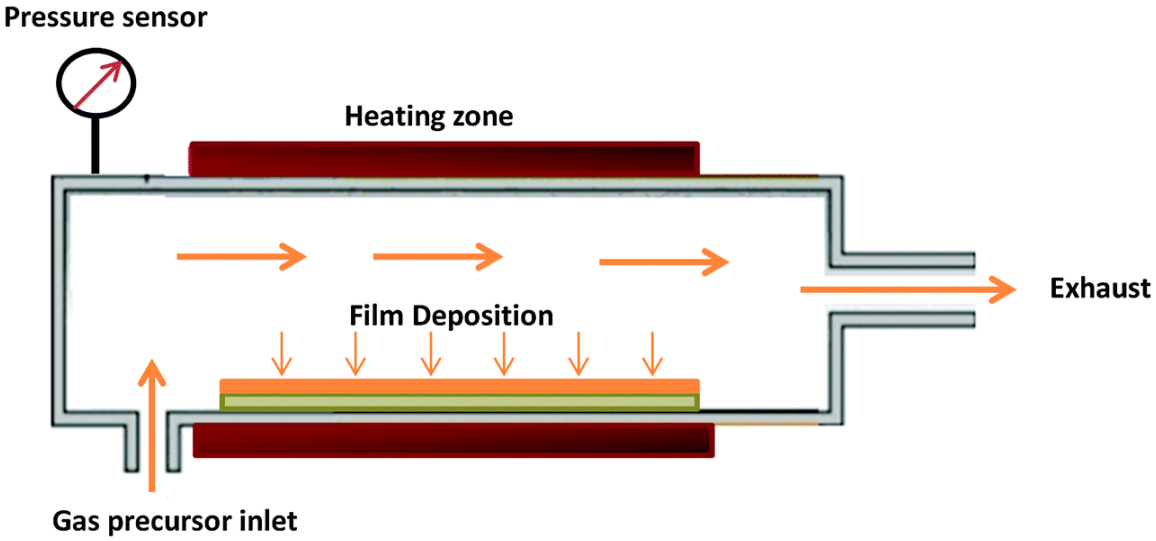

Figure 18. Schematic illustration of a CVD process. Reproduced from Zhang et al. *J. Mater. Chem. C.* **2016**, *4*, 4092-4124. Copyright 2016 Royal Society of Chemistry

In 1982, Spear developed a model of the sequential physical and chemical steps which happen during the CVD process[67,68]. Figure 19 represents the CVD model, summarized as followed:

(1) The gaseous reactant transport to the proximity of the substrate surface;

(2) The reactant species diffuse to the substrate surface through a boundary layer or intermediates are formed by homogeneous chemical reactions;

(3) The reactant species or formed intermediates are adsorbed on the substrate surface;

(4) The species migrate on the surface, the heterogeneous reaction occurs, and by-product species are formed;

(5) The by-product species are desorbed from the reaction surface;

(6) The by-product species diffuse to the bulk gas and boundary layer; and

(7) The by-product gaseous species move away from the substrate (exhaust)[69].

Since the principle of CVD processes involves depositing a new layer of material onto a substrate surface, CVD belongs to the family of additive manufacturing techniques. The advantage of the CVD process compared to other additive manufacturing techniques such as powder-based 3-D printing or laser-based deposition techniques is that the CVD does not need any external driver for the solidification process. The CVD method relies on chemical reactions occurring at the atomic level to form a strong bond for the thin layers of coating on the substrate. Hence, the CVD process can be considered an accurate micro- or nano-scale manufacturing technique[69].

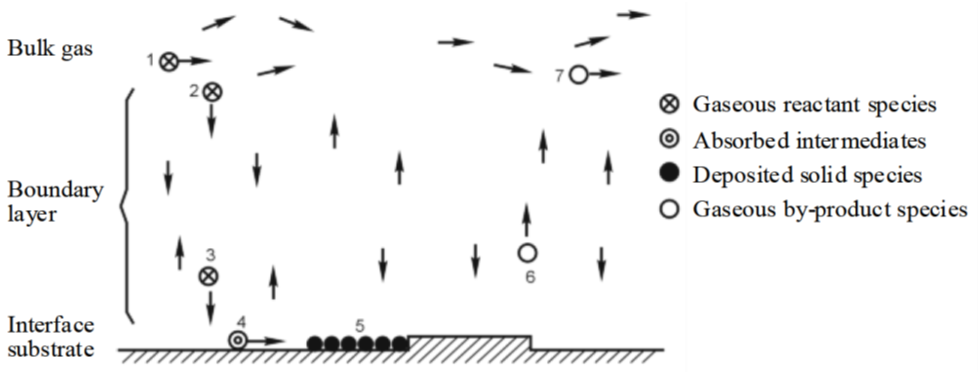

Figure 19: Schematic of the CVD model developed by Spear. Reproduced from Yan and Xu, *Chemical Vapour Deposition: AN Integrated Energineering Design for Advanced Materials*. Copyright 2010 Springer

Over the past few years, the CVD process has emerged as an important and promising method for the preparation and production of nano-sized carbon-based materials for energy conversion systems. Carbon nanotubes (CNTs) and carbon nanofibers (CNFs), considered key carbon materials in nanotechnology, have been synthesized by the CVD process and have been widely used as catalyst supports for PEMFCs in order to reduce the materials cost to lead to a reduction in system cost. Both CNTs and CNFs possess excellent conductivities, large surface areas, and structural stability[33,70,71].

CNTs have cylindrical geometry in nano scale with the diameter of 0.5-20 nm and the length up to a few centimeters. CNTs can essentially be divided into two categories: single-walled carbon nanotubes (SWCNTs) and multi-walled carbon nanotubes (MWCNTs) with relatively high

electrical conductivity. The SWCNT structure consists of a polyaromatic mono-atomic graphene sheet made of hybridized carbon atoms with a hexagonal display. MWCNTs are made of two to several tens of graphene cylinders stacked with an adjacent layer spacing of around 0.34 nm[72–74]. CNFs, as key carbon materials, have also been used as a catalyst support. Compared to CNTs, the diameter of CNFs can be larger and easily reach 500 nm. Moreover, there is no hollow cavity in the CNF structure[72]. Figure 20 shows the different types of CNTs and CNFs[75].

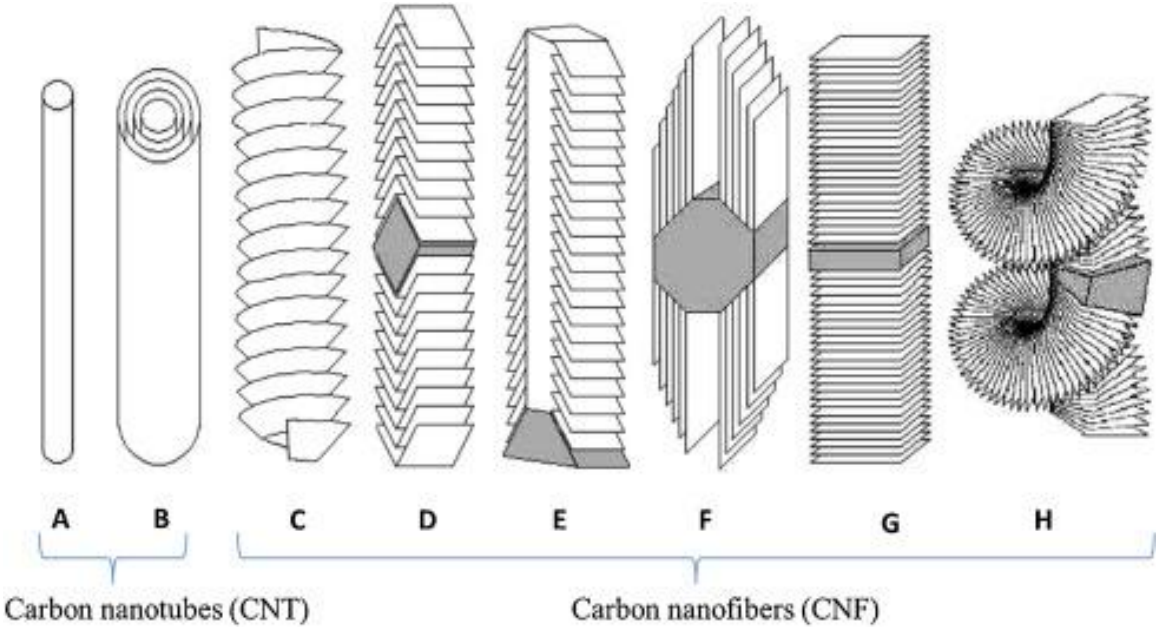

Figure 20. Different accepted structures of carbon-based fibrous nanomaterials. (A) Single-wall CNT, (B) multi-walled CNT, (C) stacked cup CNF, (D) fishbone solid CNF, (E) fishbone hollow core CNF, (F) ribbon CNF, (G) platelet CNF, (H) spiral CNF. Reproduced from Canu et al. *Int. J. Hyg. Environ. Health* **2016**, *219* (2), 166-175. Copyright 2016 Elsevier

Many studies have reported CNT growth using various CVD processes such as thermal CVD (catalytic CVD)[76], plasma-enhanced CVD (PECVD)[77], laser-assisted CVD[78], and hot-filament assisted CVD[79]. The CVD processes are considered the most effective methods for CNT fabrication due to their high scalability, variation of reactants, and high quality of the products. As an example, for the thermal CVD process, a variety of carbon sources such as hydrocarbons, carbon monoxide, and alcohol could be used as the precursor reactants[76,79,80]. The carbon source for CNT growth is decomposed in the presence of catalytic metal such as nickel, iron,

molybdenum, and cobalt. The dispersion and size of the catalytic metal on the substrates is also an important factor as the CNT diameter depends on the size of catalytic metal particles. The coating of the catalytic metals on the substrate can be controlled by the choice of using sputter pure metal films or metal-complex solutions[33,81]. In addition, research has shown that the initial stage of nucleation during the CVD process can significantly affect the quality and structure of CNTs[82,83]. Depending on the reaction chemistry and process parameters (e.g. temperature), the CVD process enables the selective production of SWCNTs or MWCNTs. The structure of the CNTs formed can be pre-determined by catalyst patterning on the substrate[84–86]. The gas-phase catalytic growth of CNTs can alternatively be performed without support material[80,87].

CNFs are also synthesized via the CVD process. The production parameters can greatly affect the structure and morphology of the synthesized CNFs. The CVD-fabricated CNFs consist of ultra-high modulus properties. As a result of the growth mechanism of CNFs, it is possible to form different wall arrangements with respect to the axis depending upon the geometry of the metallic catalyst particles and the gaseous carbon reactants (e.g. hydrocarbons or carbon monoxide)[88].

Advantages of CVD

Due to the deposition and growth mechanisms of the CVD method, there are many advantages that can be useful for the synthesis and deposition of nanomaterials for PEMFCs and PEMWEs. By modifying the CVD process parameters, it is possible to greatly impact the properties of the deposited materials such as modifying the surface morphology and crystal structure of the product. This can allow for the production of either porous or dense materials depending upon the desired application. The flexibility of the reactant precursors used for the CVD process allows for a wide variety of products that can be developed, including metals, oxides, nitrides, carbides, and sulfides.

In addition to the many types of materials and material structures that can be developed using the CVD method, another benefit to using the CVD method is the ability to fabricate uniform thin films on complex substrates. With the precursor gases filling the reaction chamber containing the substrate, the CVD method allows for uniform coatings over complex shaped components. The gas flow rate can also be adjusted to allow for more control over the deposition rate of the end products depending upon the desire for epitaxial thin films or the development of thick protective coatings.

Applications of CVD

Shao et al. investigated the electrochemical oxidation of commercial carbon black (Vulcan XC-72) and CVD synthesized MWCNTs, both widely used as catalyst supports for low-temperature PEMFC application[89]. The results revealed that the CVD synthesized MWCNTs are more resistant to electrochemical oxidation compared to the commercial Vulcan XC-72 carbon black. The increase in total surface oxygen for the Vulcan XC-72 carbon black was more significant than that of the CVD-synthesized MWCNTs during 120 h holding at 1.2 V due to the specific structure of the CVD-synthesized MWCNTs[89].

Kim and Moon prepared PEM fuel cell catalysts with improved electrochemical properties by dispersing Pt nanoparticles onto CNTs synthesized under various CVD conditions[90]. The prepared Pt/CNT catalysts showed considerably larger active sites and higher electrochemical surface area (ECSA) than that of the commercial Pt/C catalyst. The single cell performance of the Pt/CNT catalyst with 41.7 wt% Pt was also better than that of the commercial Pt/C catalyst with 40.0 wt% Pt. The higher ECSA and performance of the prepared Pt/CNT catalyst is reported to be the result of higher electrical conductivity of the CVD compared to the commercial carbon black[90].

Shaijumon et al. synthesized MWCNTs by catalytic decomposition of acetylene over $MmNi_2$ hybrid catalysts (Mm denotes mismatch metal) using a thermal CVD process[91]. Thereafter, they prepared the Pt-loaded MWCNT (Pt/MWCNT) cathode catalysts for PEMFC application via a chemical reduction method. Figure 21 shows TEM micrographs of the synthesized MWCNTs and Pt/MWCNT catalysts. The results indicated that the cathode catalyst with 50% Pt/MWCNT and 50% commercial Pt/C shows the best performance for oxygen reduction reaction (ORR) due to better dispersion and good accessibility of MWCNT support and Pt catalyst[91].

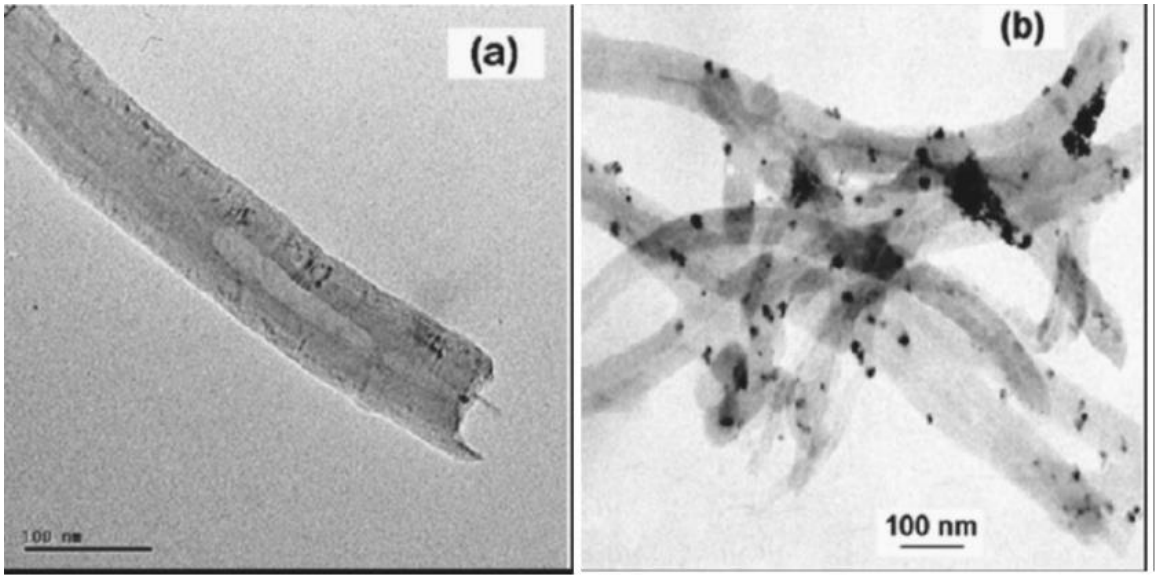

Figure 21. TEM images of (a) the CVD synthesized MWCNTs and (b) the Pt/MWCNT catalyst. Reproduced from Shaijumon et al. *Appl. Phys. Lett.* **2006**, *88* (25), 2004-2007. Copyright 2006 AIP Publishing

Tsai et al. successfully grew dense CNT on the carbon cloths using a thermal CVD process[70]. The synthesized CNTs, grown directly on the carbon cloth and used as the catalyst support for the PEM fuel cell application, improved the electrical contact between the diffusion layer and the support which leads to higher active surface area for the catalyst. They also successfully formed Pt (~4.5-9.5 nm) and Pt-Ru (~4.8-5.2 nm) nanoparticles on the synthesized CNTs using a potentiostatic electrodeposition technique. Figure 22 shows TEM micrographs of the prepared

catalysts. The electrochemical tests showed the electrodeposited Pt-Ru catalyst exhibits better mass activity for methanol oxidation.

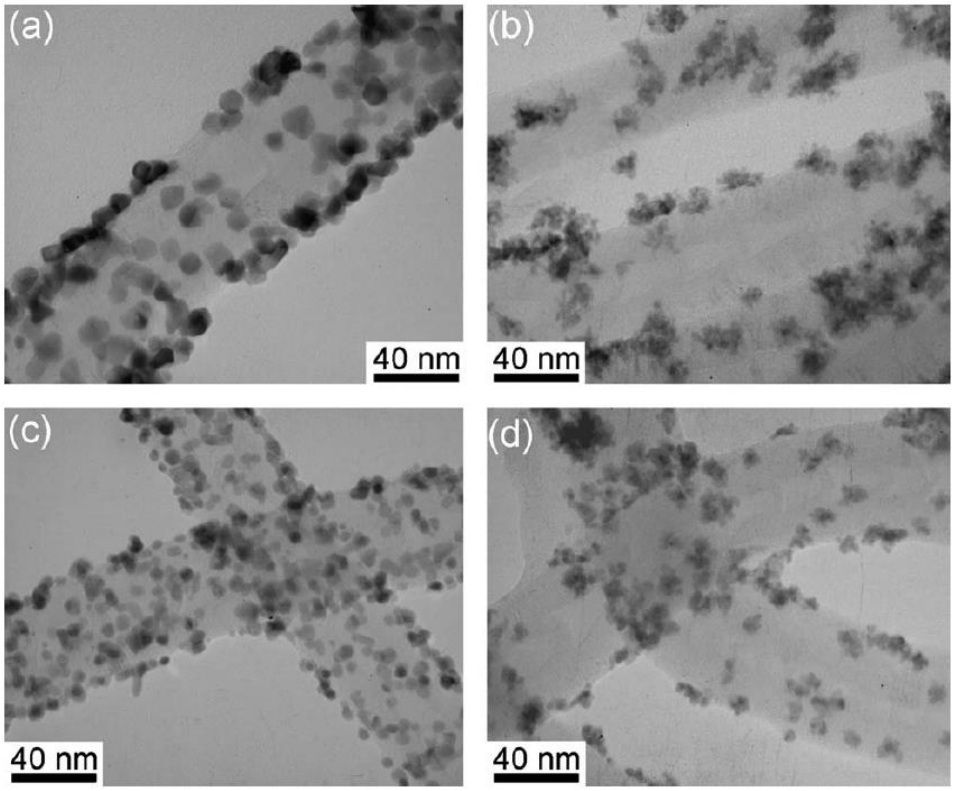

Figure 22. TEM micrographs of working specimens with Pt (a) and (c), and working specimens with Pt-Ru (b) and (d) at different catalyst loadings. Reproduced from Tsai et al. *Electrochem. Commun.* **2006**, 8 (9), 1445-1452. Copyright 2006 Elsevier

Li et al. used the CVD method for the production of CNFs[92]. The as-prepared CNF, containing Cu/Ni catalysts, phosphorous, nitrogen and boron dopants, was directly used as the catalyst support for Pt nanoparticles for PEMFCs without any functionalization as shown in Figure 23. The CNF support showed a good hydrophobicity due to the presence of P, N, and B dopants. In addition, the synthesized Pt/CNF in this work revealed high ORR activity and promising stability with 17.7% ECSA loss from 500th scan to 2000th scan during accelerated stress tests.

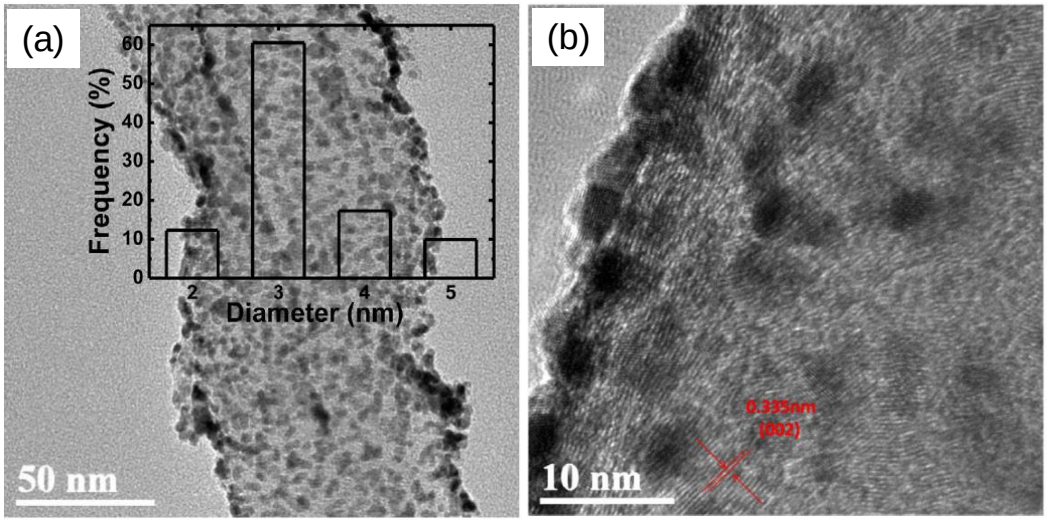

Figure 23. TEM micrographs of the synthesized Pt/CNF at two different magnifications. Reproduced from Li et al. *Electrochim. Acta* **2015**, *182*, 351-360. Copyright 2015 Elsevier

Future Development of CVD

In recent years, the CVD technique has been extensively used as promising method for the synthesis of various 1-D, 2-D, and 3-D carbon-based nanomaterials for PEM-based energy conversion applications due to their unique characteristics such as electrical conductivity, corrosion resistance, strength, and large surface area as well as their ease of fabrication. However, a key challenge to enabling industries to use the high-quality carbon nanomaterials for their current applications is large-scale production. Therefore, further research is required to explore economical methods for commercial fabrication of carbon-based nanomaterials.

Atomic Layer Deposition

Another deposition process that has been used for the development of nanoparticles for advanced MEA fabrication is atomic layer deposition (ALD). ALD is a vapor-based deposition technique that is a subset of CVD technology. Similar to the CVD process, ALD involves precursor gases passing through a reaction chamber where the substrate is heated.

However, contrary to the CVD method, which utilizes a continuous flow of precursor gases for layer growth, ALD uses a modified growth mechanism with pulsed flow of precursor gases[93–97]. With ALD, the first gaseous precursor material is pulsed into the reaction chamber until the entire surface of the substrate is covered in the first "half-reaction." During this process, a monolayer of precursor is adsorbed on the surface of the substrate. Once completely covered with precursor gases, an inert gas is flowed through the reaction chamber to remove any non-adsorbed precursor. Once purged, a second precursor material is flowed into the reaction chamber. The second precursor material then reacts with the adsorbed monolayer to produce the desired catalytic thin film. Once the reaction has proceeded to completion, the reaction chamber is purged again to remove any excess second precursor material. Once purged, the process is then cycled until the desired thickness is obtained.

While typical ALD depositions are surface controlled, many deposition parameters affect the desired end product material for the target application[93,95,98]. Some of these parameters include the substrate used, the overall ALD process parameters, and the selected precursors[98]. One parameter that will critically impact the deposit and determine whether a film or nanoparticles are formed is the substrate. The surface energy of the substrate compared to the surface energy of the deposited material will greatly impact the growth mechanism. The self-limiting growth typically characteristic of ALD is observed in the case when the surface energy of the substrate is greater than the energy of the deposited ALD material. Under those conditions, the precursor material is able to wet the entire substrate and allow for layered growth. However, if the surface energy of the substrate is less than the deposited ALD material, then Volmer-Weber island growth will occur[98]. In addition to the substrate being used, the presence of functional groups on the surface of the substrate could alter the nucleation sites which impact whether nanoparticles will form or a thin

film will be developed. As shown in Figure 24, mechanisms proposed by Setthapun et al. suggest that for a Pt ALD deposition, the presence of a hydroxyl group on the surface of the substrate after an O_2 treatment would be the primary nucleation site rather than PtO [99]. As the PtO would become reduced over time, the resulting material would be Pt nanoparticles rather than a continuous Pt film.

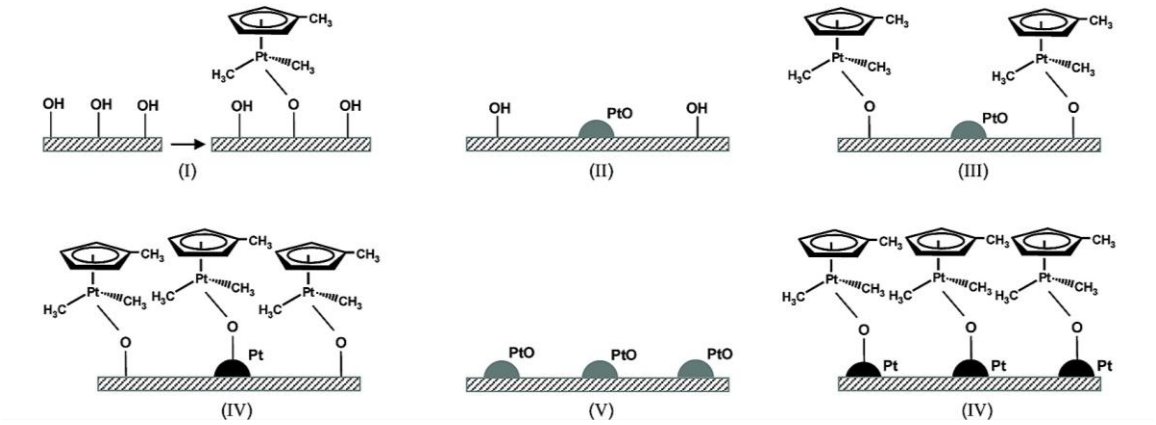

Figure 24. Proposed schemes during three cycles of Pt ALD with O_2 treatment on γ-Al_2O_3. Reproduced from Setthapun et al. *J. Phys. Chem. C* **2010**, *114* (21), 9758-9771. Copyright 2010 ACS Publications

In addition to the effect of the substrate, the specific precursor material chosen may also impact the ALD process[98]. In many sources, trimethyl(methylcyclopenadienyl) platinum (IV) ($MeCpPtMe_3$) is the traditional precursor material for Pt ALD[98–112]. However, other literature sources have examined utilizing other Pt precursor materials such as platinum acetylacetonate[98]. For this, it is important to account for the thermal stability of the precursor to obtain the desired result. Platinum acetylacetonate is not thermally stable for traditional ALD, but can be a low-cost, suitable precursor when operating under other low temperature ALD conditions.

Lastly, another major ALD parameter is related to the reactant gas flowed into the reaction chamber during the second half-reaction[98]. Traditional ALD uses oxygen gas to react with the organic ligand of the precursor material to leave the desired material on the substrate[98–101,103,104,106]. However, the use of oxygen typically requires a minimum operating temperature of 250°C. Other

researchers have used ozone as the reactant gas[98,102,105,107,108,111]. The reactivity of ozone allows for the ALD process temperature to be reduced to around 100°C while also functionalizing the surface of the substrate to improve nucleation[98]. This allows for an increase in the growth rate when using ozone.

Advantages of ALD

The unique growth mechanism of the catalyst film by ALD allows for many distinct advantages. One of the main advantages to ALD is its ability to deposit nanoscale thin films with uniform thickness. Unlike in CVD where the precursor gases are allowed to decompose in the gas-phase and on the substrate surface, which can result in nonuniform deposition thicknesses, the pulsed precursor injection associated with ALD allows for a much more uniform deposition. Due to the self-limiting growth associated with ALD, excess precursor material will not adsorb onto already-adsorbed precursor material[93]. As a result, it is possible to obtain thin films with uniform thickness regardless of substrate porosity or tortuosity. Additionally, the growth mechanism causes the thin films to be much thinner than in CVD or many other vapor-based deposition techniques with angstrom scale layer growth per cycle[93]. This can be beneficial when developing materials for PEM-based devices as a method to reduce the total PGM loading of the cell electrodes.

In addition to the uniformity of the coatings, another major benefit to utilizing ALD is the scalability of the deposition process. Since the ALD process is primarily controlled by the active surface rather than the deposition process parameters, ALD scalability is only limited by the size of the reaction chamber[93,95]. Since the precursor will only adsorb to the active surface and can be flowed into the reaction chamber until the entire surface is coated, the only limitation to the size of the deposition area is the size of substrate that can fit within the reaction chamber.

Applications of ALD for PEMFCs

One of the many challenges for PEMFC electrode development is the fabrication of electrodes with low catalyst loading while maintaining high catalyst activity. One method for obtaining Pt nanoparticles over a uniform area is with ALD. Research has demonstrated the ability of ALD to deposit Pt nanoparticles on a number of various substrates. Among those substrates are carbon catalyst supports which could be used for PEMFC applications. Recently, Liu et al. have developed an ALD process that allows Pt nanoparticles to be deposited on carbon nanotubes (CNT)[100]. The authors deposited Pt by using $MeCpPtMe_3$ as the platinum precursor and used oxygen gas as the second precursor gas. By first functionalizing the CNT surface through a nitric acid treatment process, Liu et al. was able to deposit Pt nanoparticles onto the CNT support and determined that increasing the acid treatment time resulted in high Pt loadings due to an increase in the number of functional groups on the CNT surface. Similarly, Shu et al. examined the deposition of Pt nanoparticles on CNT supports that were functionalized in a citric acid treatment process[101]. Following 100 ALD cycles, Shu et al. were able to deposit 3-5 nm Pt nanoparticles uniformly distributed on the CNT supports as determined from TEM micrographs. In order to determine the activity of the Pt ALD catalyst, Shu et al. compared MEAs developed with Pt from ALD to commercial MEAs from Johnson Matthey. The polarization curves measured from MEAs fabricated with ALD-Pt and commercial MEAs from Johnson Matthey are compared in Figure 25. According to the resulting data, Shu et al. determined that the power density of the cells developed using Pt from ALD was 2.95 kW g_{Pt}^{-1} at 80°C operation while the cells from Johnson Matthey exhibited a power density of 1.90 kW g_{Pt}^{-1} at 80°C. Additionally, the cells fabricated with ALD showed similar stability at 0.7 V steady-state operation for over 50 hours compared to the commercial cell.

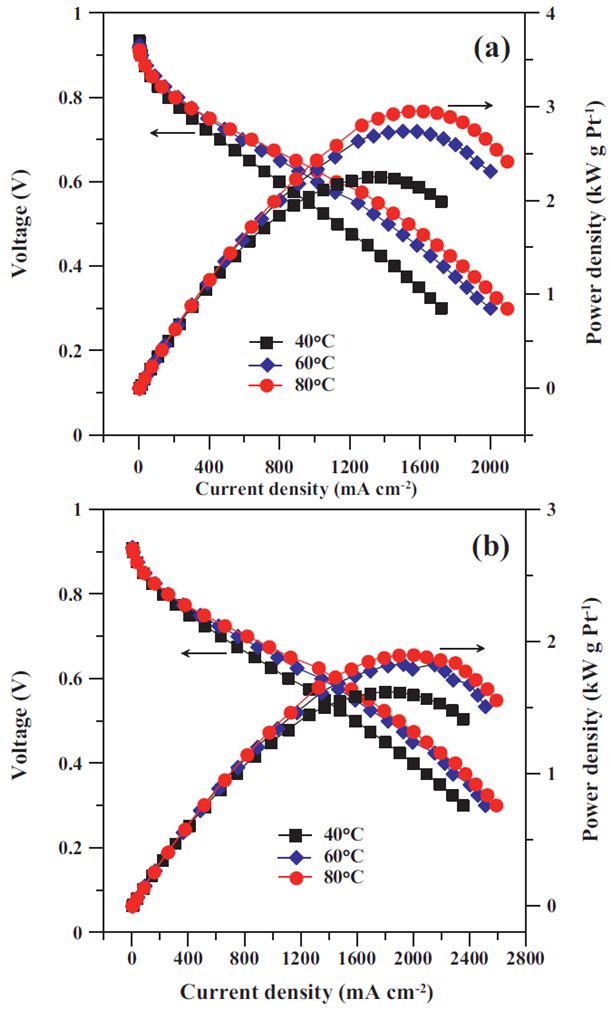

Figure 25. Polarization curves measured with MEAs assembled with (a) ALD-Pt and (b) commercial Pt (Johnson Matthey) anodes at 40, 60, and 80°C. Reproduced from Shu et al. *Electrochim. Acta* **2012**, *75*, 101-107. Copyright 2012 Elsevier

In recent years, researchers have also begun to utilize the ALD process to reduce PGM catalyst loadings in the electrodes. One way to reduce the PGM loading is to develop core-shell catalysts which non-PGM cores with catalytically active PGM shells. These core-shell catalysts utilize much less PGM material as only a thin shell is required. In addition, Baker et al. and Clancey et al. have deposited thin films on TiO_2 nanoparticles to create novel catalysts for PEM fuel cells[109,110]. In order to allow for appropriate adhesion of Pt on the TiO_2 core, thin ALD layers of Al_2O_3 and W are first deposited onto the TiO_2. With the modified surface chemistry of the

nanoparticle core, the Pt can then be deposited onto the outer W shell with uniform Pt growth. Figure 26 shows how the Pt layer thickness and Pt layer density changes with an increasing number of ALD cycles. At layer thicknesses greater than 1.5 nm, it is possible to obtain a continuous Pt film with a density greater than 95% of bulk Pt[109].

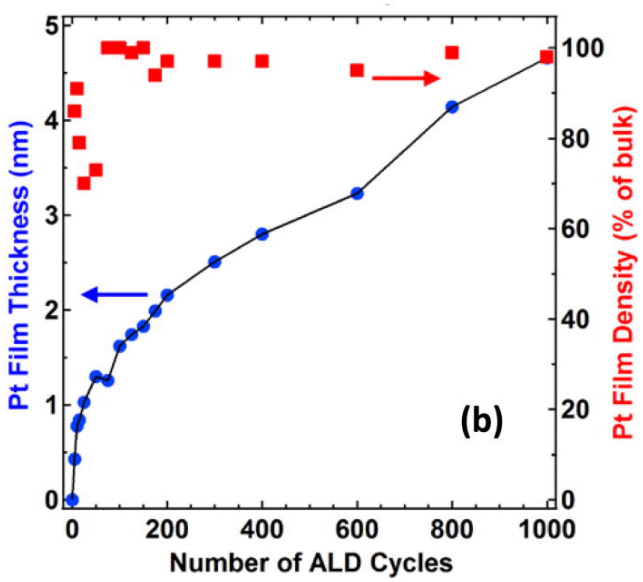

Figure 26. Pt film thicknesses and density versus number of ALD cycles on W ALD adhesion layer using $MeCpPtMe_3$ and H_2 plasma as reactants at 120°C over all 1000 ALD cycles. Reproduced from Baker et al. *Appl. Phys. Lett.* **2012**, *101* (11), 111601. Copyright 2012 AIP Publishing

Applications of ALD for PEMWEs

While the ALD method has been shown to be a feasible process for the development of Pt/C catalysts for PEMFCs, additional research has been performed in order to explore its applicability for the development of catalysts for the oxygen evolution reaction that takes place on the anode of the PEMWE. In recent years, research has begun on the development of iridium by ALD for water electrolysis applications[97,113–115]. Schlicht et al. recently reported they were able to develop an iridium deposition process using ALD[113,114]. The authors used ethylcyclopentadienyl-1,3-cyclohexadiene-iridium (I) ((EtCp)Ir(CHD)) as the first precursor material with ozone as the second precursor gas. Working with these precursors and gases, they were able to deposit Ir thin films on anodized aluminum oxide and TiO_2 nanotube supports. The electrochemical performance

of the ALD deposited Ir was then examined and determined that at 10 mA cm^{-2}, the overpotential is less than 0.24 V which is lower than other cited Ir or IrO_x developed by other techniques[114].

Similarly, work on the development of Ir thin films by ALD was performed by Matienzo et al. using iridium acetylacetonate and ozone precursors[115]. During the deposition, a growth rate of 0.53Å per cycle was estimated and an oxygen overpotential of 0.285 V was measured at 1000 mA cm^{-2}. These results confirm the feasibility of ALD to deposit thin Ir films which have high activity and can be used in future PEMWE development.

Future Development for ALD

Due to the many different components associated with the ALD process, there are many possibilities for future development. In many cases, modifications to the ALD process are being examined for improving the development of nanomaterials[116]. One study by Xu et al. modified the ALD process to obtain Pt nanoparticles with high activity by developing passivation-gas-incorporated ALD (PALD)[108]. While Xu et al. used $MeCpPtMe_3$ and ozone precursors similar to the ALD process, the primary difference with PALD is that carbon monoxide was flowed into the reaction chamber at the end of each cycle. The carbon monoxide adsorbed onto the deposited Pt nanoparticles preventing further Pt deposition at that site in the following cycles. By suppressing the thickness of the Pt nanoparticles, PALD allows for two-dimensional growth of the Pt nanoparticles, which results in a significant increase in the catalyst activity as shown in Figure 27. The catalyst activity was tested through rotating disk electrode experiments where the mass activity at 0.9 V vs. RHE was determined to be greater than 1.3 A mg_{Pt}^{-1}, which greatly exceeds the DOE target of 0.44 A mg_{Pt}^{-1}.

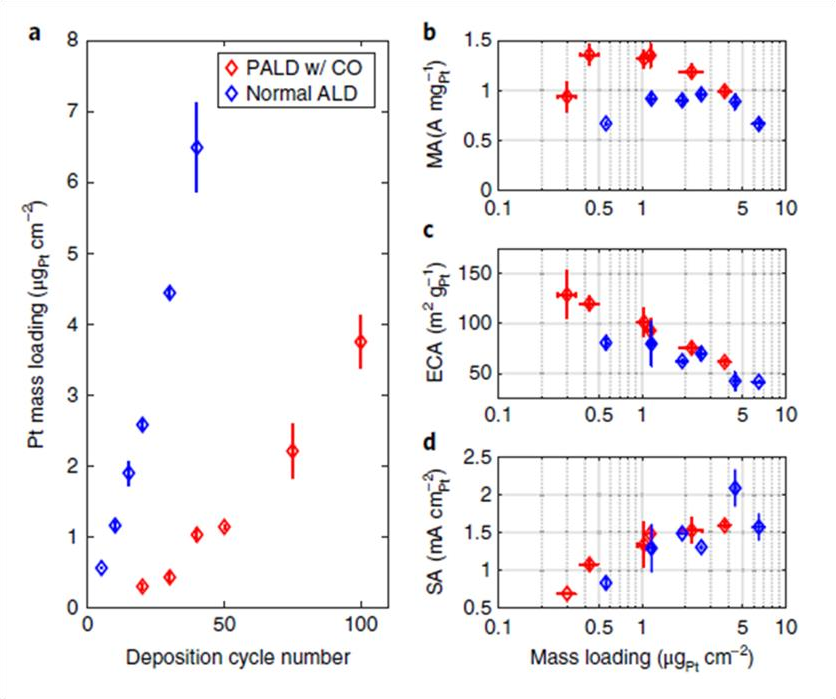

Figure 27. (a) Mass loadings of Pt deposition via ALD (blue) and PALD (red) as a function of the deposition cycle number. (b) Mass activity, (c) electrochemical surface area, and (d) specific activity of ALD and PALD samples for ORR as a function of mass loading. Reproduced from Xu et al. *Nat. Catal.* **2018**, *1*, 624-630. Copyright 2018 Springer Nature

Another modification to the ALD process that is under development is the spatial ALD (SALD) process[104,116]. With SALD, the substrate is fed through a reactor system that has distinct reaction zones separated by inert gas regions as illustrated in Figure 28. This design removes the need for distinct purging cycles and allows for high throughput catalyst development which can be used for commercialization of this fabrication technique. Research by van Ommen et al. has examined SALD for the development of catalysts with Pt nanoparticles deposited on TiO_2 using just one ALD cycle as a proof-of-concept[104]. While the research by van Ommen et al was not designed for catalyst development for PEM devices, it shows the capability of SALD to deposit Pt nanoparticles and it demonstrates, through further modifications of the SALD process, it would be possible to obtain the additional cycles required for the development of catalysts for PEM.

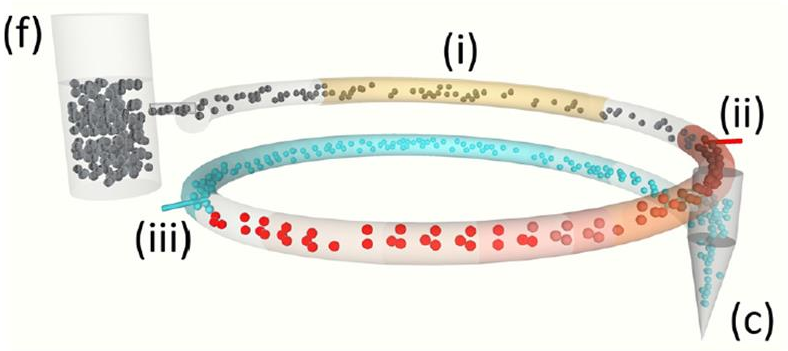

Figure 28. Schematic of the spatial ALD reactor consisting of (f) a fluidized feeding vessel, a pneumatic transport line made of three segments: (i) preheating, (ii) precursor reaction zone, (iii) co-reactant reaction zone, and (c) a collection vessel. Reproduced from van Ommen et al. *J. Vac. Sci. Technol. A Vacuum, Surfaces, Film.* **2015**, *33* (2), 021513. Copyright 2015 AVS

Another possible scale-up mechanism for the development of supported catalysts by ALD is through the use of a fluidized bed reactor. Li et al. were able to demonstrate the ability of this technology by depositing Pt nanoparticles on a silica gel powder[117]. While maintaining fluidization for the inlet precursor gases, in-situ mass spectrometry allowed Li et al. to determine when the half-reactions were completed. Results from this research showed that after 3 ALD cycles, it was possible to obtain Pt nanoparticles with an average particle size of 1.2 ± 0.3 nm with 90% dispersion on the silica support. Further development of such a technology may provide a high throughput mechanism for the development of supported catalysts for PEM technologies.

Other Vapor-based Processes

In addition to the main vapor-based processes listed above and their derivatives, there are additional catalyst synthesis and deposition techniques discussed in this section. Among those processes are plasma-based processes such as plasma enhanced chemical vapor deposition (PECVD) and magnetron sputtering[118–121]. Magnetron sputtering is capable of producing PEMFC MEAs with higher performance compared to traditional methods. Cavarroc et al. fabricated cathodes for PEMFCs with a Pt loading of 0.01 mg_{Pt} cm^{-2}, which have a specific power of 20 kW

g_{Pt}^{-1}.[119] Laurent-Brocq et al. propose another similar plasma-based method in which a low-temperature radio frequency plasma deposition process is used to synthesize Pt electrocatalysts[122]. As-synthesized Pt nanoparticles have a uniform particle size distribution of 3-4 nm and are evenly distributed on carbon supports during the plasma treatment process[122]. A recent review by Alexeeva and Fateev details additional benefits of the magnetron sputtering process as an electrocatalyst synthesis technique and provides suggestions for future advancements[121].

Another emerging nanoparticle synthesis process that could be useful for the development of electrocatalysts is spark ablation[123,124]. During the spark ablation process, electrodes are connected to an electrical circuit. The current in the circuit is oscillated at high frequencies (~1MHz) which creates a spark between the electrodes. The spark causes the electrode material to evaporate and form nanoparticles with the same composition[123]. Depending on the electrode material used and the electrical circuit parameters chosen, it is possible to control both particle size and resultant nanoparticles composition. Thus, pure metallic nanoparticles or nanoparticles with a multi-elemental composition can be synthesized by this method[123]. Lu et al. have used the spark ablation technique to synthesize pure silver nanoparticles, which were deposited directly onto carbon fibers and tested for their HER activity[124]. While this spark ablation method has many advantages, scalability may be a concern for commercial fabrication of electrocatalysts due to long deposition times. For example, Lu et al. reported the theoretical production rate of their Ag nanoparticles is around 2.4 mg hr^{-1}, which is too low and hinders its applicability in the desired large scale roll-to-roll catalyst manufacturing process[124].

Discussion

Comparison of Vapor-based Processes

Each of the vapor-based processes discussed in this review have unique advantages and disadvantages as detailed in Table 1. For example, with spray pyrolysis, operators have the capability to control both particle size and pore size depending on the desired application of the catalysts or supports. This manufacturing control allows for the development of highly active and durable catalysts. Similarly, spray pyrolysis precursors can be chosen so that the elemental composition of the desired nanoparticles can be tightly controlled. The benefits of microstructural and composition control have led to spray pyrolysis being used in commercial settings with patents being filed to allow for high throughput fabrication of electrocatalysts. Despite these positives, one disadvantage of spray pyrolysis is that it is an energy-intensive process that requires a significant amount of added heat to decompose the precursor materials to the desired catalyst nanoparticles. With furnaces set to operate between 300-700°C, a significant amount of energy is required to produce the desired electrocatalysts which can lead to a costly process. This high temperature operation also requires additional processing steps so that the fabricated catalyst can be deposited onto the desired membrane or GDL for application in PEM-based electrochemical devices.

While simultaneous catalyst synthesis and thin film deposition may not be possible for PEM-based devices with spray pyrolysis, it is a major advantage for the RSDT process. By incorporating an air quench, the RSDT process is able to control the substrate temperature so that the electrocatalysts being synthesized in the RSDT flame can be directly deposited onto membranes to create MEAs in one step. In addition to the ability to directly deposit the catalysts onto membranes and other temperature-sensitive substrates, the RSDT process has similar advantages to spray pyrolysis. By adjusting RSDT parameters, it is possible to precisely control the particle size of the nanoparticles while adjusting the precursor solution composition can allow for control of the elemental composition of the desired catalyst. One of the main disadvantages of the RSDT

process at this time is the scalability of the process. Further improvements in this technology are required in order to reduce the fabrication time of large scale MEAs, as well as to increase the overall efficiency of the deposition process.

CVD and ALD both have similar advantages and disadvantages. One of the main advantages to using CVD and ALD are that both allow for the deposition of uniform coatings. Due to the unique deposition process, it is possible to develop thin films with a specified thickness over complex structures. By limiting the amount of excess material deposited with CVD or ALD, it is possible to reduce the catalyst loadings when using these deposition processes. However, CVD and ALD are ultra-high vacuum techniques, and both are limited by the size of the reactor which will limit their use in commercial catalyst synthesis and deposition. In addition, both methodologies require long deposition times due to their deposition mechanism.

Table 1. Comparison of Vapor-based Techniques

Process	Advantages	Disadvantages
Spray Pyrolysis	• Particle-size control • Pore-size control • Catalyst Composition Control	• Secondary Processing Required for MEA Fabrication • Furnace Required
Reactive Spray Deposition Technology (RSDT)	• Particle Size Control • Catalyst Composition Control • One Step Catalyst Synthesis and Deposition • Electrode Morphology Control • Open Atmosphere Operation	• Small-Scale Operation • Deposition Efficiency
Chemical Vapor Deposition (CVD)	• Precursor Flexibility • Catalyst Morphology Control • Controlled Uniform Thickness	• High Vacuum Required • Limited Scalability
Atomic Layer Deposition (ALD)	• Precursor Flexibility • Catalyst Morphology Control • Controlled Uniform Thickness	• High Vacuum Required • Limited Scalability

<u>Comparison to Traditional Processes</u>

While it is important to be able to compare the vapor-based processes to one another, it is also important to compare those processes with current manufacturing processes. As previously mentioned, two common methods for commercial MEA fabrication are screen printing and decal transfer. While both of these processes have been demonstrated at an industrial scale and have demonstrated high performance suitable for commercial use, there are a few disadvantages that must be addressed. For example, screen printing can be a time-consuming process due to multiple ink application and drying steps and decal transfer requires a hot-pressing step that can potentially result in microstructural changes to the catalyst layer. In addition, it is important to note that both methods exclude the catalyst synthesis step, which is time-consuming and adds to the overall time for the MEA fabrication while the vapor-based methods include material synthesis. Furthermore, while screen printing and decal transfer have both led to a decrease in catalyst loading, the catalysts developed by vapor-based processes have allowed for particle size and pore size modifications, which results in improved MEA performance operation with even lower catalyst loadings.

The roll-to-roll manufacturing technique is seen as the primary method for industrial-scale MEA fabrication. One of the major benefits of roll-to-roll manufacturing is the ability to create large MEAs in a short period of time. Analysis has shown that, in order to meet the expecteddemand for PEMFC MEAs, MEAs need to be produced at a rate of 20 m^2 min^{-1}.[125] Roll-to-roll manufacturing is expected to reach that production rate. However, roll-to-roll manufacturing faces many challenges. Mauger et al. demonstrated a roll-to-roll process with catalyst ink applied to the membrane using gravure rollers[125]. Results showed that the speed of the roll-to-roll components will impact the uniformity of the layer with a higher ratio of gravure cylinder speed to web speed resulting in a more uniform layer.[125] However, this higher speed ratio also results in a higher catalyst loading (~0.12 mg_{Pt} cm^{-2}). This catalyst loading is similar to what has been obtained with

vapor-based processes. Additionally, the roll-to-roll manufacturing method has shown to have lower catalyst activity compared to other processes. Mauger et al. reported that the roll-to-roll process demonstrated an ORR mass activity of a Pt/HSC catalyst as 322 ± 38 mA mg_{Pt}^{-1} at 0.9V when operating at 80°C, 100% relative humidity, and 150 kPa[125]. Compared to the RSDT process, Yu et al. reported an ORR mass activity of a Pt/KB catalyst as 510 mA mg_{Pt}^{-1} at 0.9V when operating at 80°C, 100% relative humidity, 280 kPa with a similar catalyst loading as the roll-to-roll MEA examined by Mauger et al[47]. While the RSDT is not currently capable of operating at the industrial-scale, its open atmosphere operation allows for the RSDT process to potentially be incorporated into roll-to-roll manufacturing in the future.

Conclusions

While there have been significant research efforts over the years with the intent of improving the performance of the PEMFCs and PEMWEs, there also needs to be research that examines the manufacturing techniques used to fabricate nanomaterials for these PEM-based systems. With improvements to the current manufacturing methods, it is possible to make both PEMFCs and PEMWEs more economically feasible by reducing the PGM catalyst loadings, improving catalyst activity, and improving the scalability of the manufacturing techniques. Vapor-based manufacturing techniques, such as spray pyrolysis, RSDT, CVD, and ALD all have the capability of fabricating advanced nanomaterials that can boost the commercialization of PEMFCs and PEMWEs.

Literature sources have demonstrated that each of the reviewed vapor-based catalyst synthesis methods have the ability to produce nanomaterials that improve upon the performance of current state-of-the-art catalysts. Many of these performance improvements can be attributed to the

physical properties of the deposited materials that can be tuned using these unique synthesis methods. For example, by improving the distribution of the PGM nanoparticles on the catalyst supports by using the spray pyrolysis method[22] and developing novel catalyst supports by the CVD technique[91], catalyst performance improvements have been achieved. Also, through the fabrication of non-PGM catalysts with the spray pyrolysis method[25,26] or the development of thin Pt layers on non-PGM supports from ALD[109,110], vapor-based methods have shown the ability to create cost-effective catalysts for PEM-based systems. Lastly, literature has shown that the vapor-based methods can improve MEA fabrication methods by combining catalyst synthesis and deposition into one step, which enables the direct fabrication of catalyst layers on PFSA membranes at open air conditions, as demonstrated by the RSDT process[46,52].

Despite recent advances made in the vapor-based synthesis and deposition techniques, future development of these methods needs to examine the ability to scale up the processes to assist in the overall cost reduction of PEM-based systems. With spray pyrolysis, the process temperature remains too high for the direct deposition of the fabricated catalysts onto the desired end substrate. This requires the use of costly traditional deposition techniques to fabricate MEAs. Similarly, the catalyst materials synthesized by the CVD and ALD methods require traditional deposition methods for MEA fabrication. Meanwhile, RSDT has the ability to directly deposit the desired catalysts onto MEAs in one step.

In general, there has been significant research examining the development and optimization of vapor-based catalyst synthesis and deposition techniques in recent years. Each technique has shown significant improvements in catalyst performance compared to traditional catalyst synthesis methods while additional research is required to improve the scalability of each technique which

will allow for a widespread use of these vapor-based processes in the development of PEM-based systems.

AUTHOR INFORMATION

Corresponding Author

*Corresponding author: Ryan J. Ouimet; E-mail address: ryan.ouimet@uconn.edu

Author Contributions

The manuscript was written through contributions of all authors. All authors have given approval to the final version of the manuscript.

Funding Sources

The authors would like to respectfully acknowledge the U.S. Department of Energy, Office of Energy Efficiency and Renewable Energy for financial support of this work (award number: DE-EE0008427).

ACKNOWLEDGMENT

The authors would like to respectfully acknowledge the U.S. Department of Energy, Office of Energy Efficiency and Renewable Energy for financial support of this work (award number: DE-EE0008427). The authors would also like to sincerely thank the University of Connecticut. The content is solely the responsibility of the authors and does not necessarily represent the official views of the U.S. Department of Energy.

ABBREVIATIONS

AEMFC, Alkaline Exchange Membrane Fuel Cell; ALD, Atomic Layer Deposition; ATO, Antimony-Doped Tin Oxide; CNF, Carbon Nanofiber; CNT, Carbon Nanotube; CVD, Chemical Vapor Deposition; ECSA, Electrochemical Surface Area; FSP, Flame Spray Pyrolysis; GDL, Gas Diffusion Layer; LFL, Lower Flammability Limit; MEA, Membrane Electrode Assembly; MWCNT, Multi-walled Carbon Nanotube; OER, Oxygen Evolution Reaction; ORR, Oxygen Reduction Reaction; PALD, Passivation-gas-incorporated Atomic Layer Deposition; PECVD, Plasma-enhanced Chemical Vapor Deposition; PEM, Proton Exchange Membrane; PEMFC, Proton Exchange Membrane Fuel Cell; PEMWE, Proton Exchange Membrane Water Electrolysis; PFSA, Perfluorosulfonic Acid; PGM, Platinum Group Metal; PTL, Porous Transport Layer; RDE, Rotating Disk Electrode; RSDT, Reactive Spray Deposition Technology; SALD, Spatial Atomic Layer Deposition; SWCNT, Single-walled Carbon Nanotube.

AUTHOR BIOGRAPHIES

Mr. Ryan J. Ouimet received his B.S.Eng. in Chemical Engineering from the University of Connecticut in 2014. He is currently a graduate research assistant at the University of Connecticut where he will receive his Ph.D. in 2021. He is also currently a research scientist at Nel Hydrogen. Mr. Ouimet's research interests include the synthesis and development of novel catalysts for fuel cell and electrolyzer technologies.

Mr. Thomas A. Ebaugh received his B.S. in Chemical Engineering from Lehigh University in 2015. He is currently enrolled as a graduate research assistant in the Ph.D. program in the Department of Chemical and Biomolecular Engineering at the University of Connecticut. Mr.

Ebaugh's research interests include fuel cells, flow batteries, gas sensors, and flame-based fabrication processes.

Dr. Gholamreza Mirshekari received his Ph.D. in Engineering from Tennessee Technological University in 2018. In 2019, he joined the University of Connecticut as a Postdoc. He currently is an Electrode Process Engineer at Alchemr, Inc., leading the development of electrode manufacturing processes for at-scale production. Dr. Mirshekari's research interest is in the development of electrochemical energy conversion devices with a focus on design, fabrication, and characterization of catalysts and electrodes for fuel cells and electrolyzers.

Dr. Stoyan Bliznakov received his Ph.D. degree in Electrochemistry from the Bulgarian Academy of Sciences in 2007. Currently, he is an Associate Research Professor at the Center for Clean Energy Engineering at the University of Connecticut. Dr. Bliznakov's research interests are in the development of advanced electrochemical energy storage and conversion devices, including PEM fuel cells, electrolyzers, and batteries. Dr. Bliznakov is a co-author of 65 peer-reviewed papers, two book chapters, and holds four US patents.

Mr. Leonard J. Bonville (Bachelor of Physics, Iona College 1964) is a Research Specialist at the University of Connecticut focusing on catalyst fabrication and testing for performance and stability. Previously, Mr. Bonville was Vice President of Engineering at International Fuel Cell (IFC), Division of United Technologies. As of VP Engineering, he managed the development and application of IFC fuel cells for the manufacturing of fuel cell products. Mr. Bonville has more than 70 publications and 15 patents.

Dr. Radenka Maric received her PhD from Kyoto University. She is Vice President for Research, Innovation and Entrepreneurship at UConn and UConn Health, and is the CT Clean Energy Fund

Professor of Sustainable Energy in the Departments of Chemical & Biomolecular Engineering and Materials Science & Engineering. Dr. Maric is an entrepreneur and leading scientist with experience in academia, industry, national labs, and federal agencies in the US, Japan, and Canada. She is an NAI and AAAS Fellow.

REFERENCES

(1) Bennett, S.; Remme, U. *The Future of Hydrogen*; International Energy Agency: Paris, 2019.

(2) Acar, C.; Dincer, I. Review and Evaluation of Hydrogen Production Options for Better Environment. *Journal of Cleaner Production* **2019**, *218*, 835–849. https://doi.org/10.1016/j.jclepro.2019.02.046.

(3) De las Heras, A.; Vivas, F. J.; Segura, F.; Andújar, J. M. From the Cell to the Stack. A Chronological Walk through the Techniques to Manufacture the PEFCs Core. *Renewable and Sustainable Energy Reviews* **2018**, *96*, 29–45. https://doi.org/10.1016/j.rser.2018.07.036.

(4) Ayers, K. The Potential of Proton Exchange Membrane–Based Electrolysis Technology. *Current Opinion in Electrochemistry* **2019**, *18*, 9–15. https://doi.org/10.1016/j.coelec.2019.08.008.

(5) Ajanovic, A.; Haas, R. Economic and Environmental Prospects for Battery Electric- and Fuel Cell Vehicles: A Review. *Fuel Cells* **2019**, *19* (5), 515–529. https://doi.org/10.1002/fuce.201800171.

(6) Manoharan, Y.; Hosseini, S. E.; Butler, B.; Alzhahrani, H.; Senior, B. T. F.; Ashuri, T.; Krohn, J. Hydrogen Fuel Cell Vehicles; Current Status and Future Prospect. *Applied Sciences* **2019**, *9* (11), 2296. https://doi.org/10.3390/app9112296.

(7) Hydrogen Benefits and Considerations. United States Department of Energy. https://www.afdc.energy.gov/fuels/hydrogen_benefits.html.

(8) Ayers, K.; Danilovic, N.; Ouimet, R.; Carmo, M.; Pivovar, B.; Bornstein, M. Perspectives on Low-Temperature Electrolysis and Potential for Renewable Hydrogen at Scale. *Annu. Rev. Chem. Biomol. Eng.* **2019**, *10* (1), 219–239. https://doi.org/10.1146/annurev-chembioeng-060718-030241.

(9) Wang, Y.-J.; Long, W.; Wang, L.; Yuan, R.; Ignaszak, A.; Fang, B.; Wilkinson, D. P. Unlocking the Door to Highly Active ORR Catalysts for PEMFC Applications: Polyhedron-Engineered Pt-Based Nanocrystals. *Energy Environ. Sci.* **2018**, *11* (2), 258–275. https://doi.org/10.1039/C7EE02444D.

(10) Reier, T.; Oezaslan, M.; Strasser, P. Electrocatalytic Oxygen Evolution Reaction (OER) on Ru, Ir, and Pt Catalysts: A Comparative Study of Nanoparticles and Bulk Materials. *ACS Catal.* **2012**, *2* (8), 1765–1772. https://doi.org/10.1021/cs3003098.

(11) Whiston, M. M.; Azevedo, I. L.; Litster, S.; Whitefoot, K. S.; Samaras, C.; Whitacre, J. F. Expert Assessments of the Cost and Expected Future Performance of Proton Exchange Membrane Fuel Cells for Vehicles. *Proc Natl Acad Sci USA* **2019**, *116* (11), 4899–4904. https://doi.org/10.1073/pnas.1804221116.

(12) Wilson, A.; Kleen, G.; Papageorgopoulos, D. *Fuel Cell System Cost - 2017*; DOE Hydrogen and Fuel Cells Program Record; 17007; United States Department of Energy, 2017.

(13) Taylor, A. D.; Kim, E. Y.; Humes, V. P.; Kizuka, J.; Thompson, L. T. Inkjet Printing of Carbon Supported Platinum 3-D Catalyst Layers for Use in Fuel Cells. *Journal of Power Sources* **2007**, *171* (1), 101–106. https://doi.org/10.1016/j.jpowsour.2007.01.024.

(14) Kun-Ho Kim; Lee, K.-Y.; Kim, H.-J.; Cho, E.; Lee, S.-Y.; Lim, T.-H.; Yoon, S. P.; Hwang, I. C.; Jang, J. H. The Effects of Nafion® Ionomer Content in PEMFC MEAs Prepared by a Catalyst-Coated Membrane (CCM) Spraying Method. *International Journal of Hydrogen Energy* **2010**, *35* (5), 2119–2126. https://doi.org/10.1016/j.ijhydene.2009.11.058.

(15) Leng, J.; Wang, Z.; Wang, J.; Wu, H.-H.; Yan, G.; Li, X.; Guo, H.; Liu, Y.; Zhang, Q.; Guo, Z. Advances in Nanostructures Fabricated *via* Spray Pyrolysis and Their Applications in Energy Storage and Conversion. *Chem. Soc. Rev.* **2019**, *48* (11), 3015–3072. https://doi.org/10.1039/C8CS00904J.

(16) Perednis, D.; Gauckler, L. J. Thin Film Deposition Using Spray Pyrolysis. *J Electroceram* **2005**, *14* (2), 103–111. https://doi.org/10.1007/s10832-005-0870-x.

(17) Guild, C.; Biswas, S.; Meng, Y.; Jafari, T.; Gaffney, A. M.; Suib, S. L. Perspectives of Spray Pyrolysis for Facile Synthesis of Catalysts and Thin Films: An Introduction and Summary of Recent Directions. *Catalysis Today* **2014**, *238*, 87–94. https://doi.org/10.1016/j.cattod.2014.03.056.

(18) Messing, G. L.; Zhang, S.-C.; Jayanthi, G. V. Ceramic Powder Synthesis by Spray Pyrolysis. *Journal of the American Ceramic Society* **1993**, *76* (11), 2707–2726. https://doi.org/10.1111/j.1151-2916.1993.tb04007.x.

(19) Hampden-Smith, M. J.; Kodas, T. T.; Atanassov, P.; Kunze, K.; Napolitano, P.; Bhatia, R.; Dericotte, D. E.; Atanassova, P. Electrocatalyst Powders, Methods for Producing Powders and Devices Fabricated from Same. US 6,967,183 B2, November 22, 2005.

(20) Serov, A.; Martinez, U. A.; Atanassov, P. B. Metal-Oxide Catalysts for Fuel Cells. US 9,666,877 B2, May 30, 2017.

(21) Ye, Z.; Yang, J.; Li, B.; Shi, L.; Ji, H.; Song, L.; Xu, H. Amorphous Molybdenum Sulfide/Carbon Nanotubes Hybrid Nanospheres Prepared by Ultrasonic Spray Pyrolysis for Electrocatalytic Hydrogen Evolution. *Small* **2017**, *13* (21), 1700111. https://doi.org/10.1002/smll.201700111.

(22) Böhm, D.; Beetz, M.; Schuster, M.; Peters, K.; Hufnagel, A. G.; Döblinger, M.; Böller, B.; Bein, T.; Fattakhova-Rohlfing, D. Efficient OER Catalyst with Low Ir Volume Density Obtained by Homogeneous Deposition of Iridium Oxide Nanoparticles on Macroporous Antimony-Doped Tin Oxide Support. *Adv. Funct. Mater.* **2020**, *30* (1), 1906670. https://doi.org/10.1002/adfm.201906670.

(23) Lee, J.; Kim, I.; Park, S. Boosting Stability and Activity of Oxygen Evolution Catalyst in Acidic Medium: Bimetallic Ir−Fe Oxides on Reduced Graphene Oxide Prepared through Ultrasonic Spray Pyrolysis. *ChemCatChem* **2019**, *11* (11), 2615–2623. https://doi.org/10.1002/cctc.201900287.

(24) Wang, M.; He, X.; Fang, J.; Hu, L.; Huang, H.; Liu, Z.; Lai, Y.; Liu, Y.; Zhang, J. Sacrificial Template Induced Interconnected Bubble-like N-Doped Carbon Nanofoam as a PH-Universal Electrocatalyst for an Oxygen Reduction Reaction. *Inorg. Chem. Front.* **2019**, *6* (2), 621–629. https://doi.org/10.1039/C8QI01271G.

(25) Kwong, W. L.; Lee, C. C.; Shchukarev, A.; Messinger, J. Cobalt-Doped Hematite Thin Films for Electrocatalytic Water Oxidation in Highly Acidic Media. *Chem. Commun.* **2019**, *55* (34), 5017–5020. https://doi.org/10.1039/C9CC01369E.

(26) Kwong, W. L.; Lee, C. C.; Shchukarev, A.; Björn, E.; Messinger, J. High-Performance Iron (III) Oxide Electrocatalyst for Water Oxidation in Strongly Acidic Media. *Journal of Catalysis* **2018**, *365*, 29–35. https://doi.org/10.1016/j.jcat.2018.06.018.

(27) Kim, I. G.; Nah, I. W.; Oh, I.-H.; Park, S. Crumpled RGO-Supported Pt-Ir Bifunctional Catalyst Prepared by Spray Pyrolysis for Unitized Regenerative Fuel Cells. *Journal of Power Sources* **2017**, *364*, 215–225. https://doi.org/10.1016/j.jpowsour.2017.08.015.

(28) Košević, M. G.; Zarić, M. M.; Stopić, S. R.; Stevanović, J. S.; Weirich, T. E.; Friedrich, B. G.; Panić, V. V. Structural and Electrochemical Properties of Nesting and Core/Shell Pt/TiO2 Spherical Particles Synthesized by Ultrasonic Spray Pyrolysis. *Metals* **2020**, *10* (1), 11. https://doi.org/10.3390/met10010011.

(29) Tsai, S. C.; Song, Y. L.; Tsai, C. S.; Yang, C. C.; Chiu, W. Y.; Lin, H. M. Ultrasonic Spray Pyrolysis for Nanoparticles Synthesis. *Journal of Materials Science* **2004**, *39* (11), 3647–3657. https://doi.org/10.1023/B:JMSC.0000030718.76690.11.

(30) Alkan, G.; Diaz, F.; Matula, G.; Stopic, S.; Friedrich, B. Scaling up of Nanopowder Collection in the Process of Ultrasonic Spray Pyrolysis. *World of Metallurgy* **2017**, *70* (2), 5–9.

(31) Stopic, S.; Rudolf, R.; Bogovic, J.; Majerič, P.; Colić, M.; Tomić, S.; Jenko, M.; Friedrich, B. Synthesis of Au Nanoparticles Prepared with Ultrasonic Spray Pyrolysis and Hydrogen Reduction. *Mater. Tehnol.* **2013**, *47* (5), 577–583.

(32) Alkan, G.; Rudolf, R.; Bogovic, J.; Jenko, D.; Friedrich, B. Structure and Formation Model of Ag/TiO2 and Au/TiO2 Nanoparticles Synthesized through Ultrasonic Spray Pyrolysis. *Metals* **2017**, *7* (10), 389. https://doi.org/10.3390/met7100389.

(33) Maric, R. Spray-Based and CVD Processes for Synthesis of Fuel Cell Catalysts and Thin Catalyst Layers. In *PEM Fuel Cell Electrocatalysts and Catalyst Layers*; Zhang, J., Ed.; Springer London: London, 2008; pp 917–963. https://doi.org/10.1007/978-1-84800-936-3_20.

(34) Hampden-Smith, M.; Atanassova, P.; Atanassov, P.; Kodas, T. Manufacture of Electrocatalyst Powders by a Spray-Based Production Platform. In *Handbook of Fuel Cells*; Vielstich, W., Lamm, A., Gasteiger, H. A., Yokokawa, H., Eds.; John Wiley & Sons, Ltd: Chichester, UK, 2010; p f303044. https://doi.org/10.1002/9780470974001.f303044.

(35) Serov, A.; Robson, M. H.; Smolnik, M.; Atanassov, P. Tri-Metallic Transition Metal–Nitrogen–Carbon Catalysts Derived by Sacrificial Support Method Synthesis. *Electrochimica Acta* **2013**, *109*, 433–439. https://doi.org/10.1016/j.electacta.2013.07.104.

(36) Serov, A.; Artyushkova, K.; Atanassov, P. Fe-N-C Oxygen Reduction Fuel Cell Catalyst Derived from Carbendazim: Synthesis, Structure, and Reactivity. *Advanced Energy Materials* **2014**, *4* (10), 1301735. https://doi.org/10.1002/aenm.201301735.

(37) Teoh, W. Y.; Amal, R.; Mädler, L. Flame Spray Pyrolysis: An Enabling Technology for Nanoparticles Design and Fabrication. *Nanoscale* **2010**, *2* (8), 1324. https://doi.org/10.1039/c0nr00017e.

(38) Chen, H.; Mulmudi, H. K.; Tricoli, A. Flame Spray Pyrolysis for the One-Step Fabrication of Transition Metal Oxide Films: Recent Progress in Electrochemical and Photoelectrochemical Water Splitting. *Chinese Chemical Letters* **2020**, *31* (3), 601–604. https://doi.org/10.1016/j.cclet.2019.05.016.

(39) Strobel, R.; Baiker, A.; Pratsinis, S. E. Aerosol Flame Synthesis of Catalysts. *Advanced Powder Technology* **2006**, *17* (5), 457–480. https://doi.org/10.1163/156855206778440525.

(40) Ernst, F. O.; Büchel, R.; Strobel, R.; Pratsinis, S. E. One-Step Flame-Synthesis of Carbon-Embedded and -Supported Platinum Clusters. *Chem. Mater.* **2008**, *20* (6), 2117–2123. https://doi.org/10.1021/cm702023n.

(41) Dahl, P. I.; Thomassen, M. S.; Colmenares, L. C.; Barnett, A. O.; Lomas, S.; Vullum, P. E.; Hanetho, S. M.; Mokkelbost, T. Flame Spray Pyrolysis of Electrode Materials for Energy Applications. *MRS Proc.* **2015**, *1747*, mrsf14-1747-hh05-10. https://doi.org/10.1557/opl.2015.340.

(42) Dahl, P. I.; Colmenares, L. C.; Barnett, A. O.; Lomas, S.; Vullum, P. E.; Kvello, J. H.; Tolchard, J. R.; Hanetho, S. M.; Mokkelbost, T. Flame Spray Pyrolysis of Tin Oxide-Based Pt Catalysts for PEM Fuel Cell Applications. *MRS Adv.* **2017**, *2* (28), 1505–1510. https://doi.org/10.1557/adv.2017.104.

(43) Yu, H.; Baricci, A.; Bisello, A.; Casalegno, A.; Guetaz, L.; Bonville, L.; Maric, R. Strategies to Mitigate Pt Dissolution in Low Pt Loading Proton Exchange Membrane Fuel Cell: I. A Gradient Pt Particle Size Design. *Electrochimica Acta* **2017**, *247*, 1155–1168. https://doi.org/10.1016/j.electacta.2017.07.093.

(44) Yu, H.; Baricci, A.; Casalegno, A.; Guetaz, L.; Bonville, L.; Maric, R. Strategies to Mitigate Pt Dissolution in Low Pt Loading Proton Exchange Membrane Fuel Cell: II. A Gradient Pt Loading Design. *Electrochimica Acta* **2017**, *247*, 1169–1179. https://doi.org/10.1016/j.electacta.2017.06.145.

(45) Yu, H.; Roller, J. M.; Kim, S.; Wang, Y.; Kwak, D.; Maric, R. One-Step Deposition of Catalyst Layers for High Temperature Proton Exchange Membrane Fuel Cells (PEMFC). *J. Electrochem. Soc.* **2014**, *161* (5), F622. https://doi.org/10.1149/2.045405jes.

(46) Maric, R. UConn Developing Production Method for Next-Gen PEMFCs. *Fuel Cells Bulletin* **2012**, *2012* (4), 15. https://doi.org/10.1016/S1464-2859(12)70115-3.

(47) Yu, H.; Baricci, A.; Roller, J.; Wang, Y.; Casalegno, A.; Mustain, W. E.; Maric, R. Ultra-Low Pt Loading Catalyst Layers for PEMFC Using Reactive Spray Deposition Technology. *ECS Transactions* **2015**, *69* (17), 487–496. https://doi.org/10.1149/06917.0487ecst.

(48) Yu, H.; Bonville, L.; Maric, R. Analysis of H_2/Air Polarization Curves: The Influence of Low Pt Loading and Fabrication Process. *J. Electrochem. Soc.* **2018**, *165* (5), F272–F284. https://doi.org/10.1149/2.0261805jes.

(49) Yu, H.; Danilovic, N.; Wang, Y.; Willis, W.; Poozhikunnath, A.; Bonville, L.; Capuano, C.; Ayers, K.; Maric, R. Nano-Size IrOx Catalyst of High Activity and Stability in PEM Water Electrolyzer with Ultra-Low Iridium Loading. *Applied Catalysis B: Environmental* **2018**, *239*, 133–146. https://doi.org/10.1016/j.apcatb.2018.07.064.

(50) Roller, J.; Renner, J.; Yu, H.; Capuano, C.; Kwak, T.; Wang, Y.; Carter, C. B.; Ayers, K.; Mustain, W. E.; Maric, R. Flame-Based Processing as a Practical Approach for Manufacturing Hydrogen Evolution Electrodes. *Journal of Power Sources* **2014**, *271*, 366–376. https://doi.org/10.1016/j.jpowsour.2014.08.013.

(51) Ayers, K. E.; Renner, J. N.; Danilovic, N.; Wang, J. X.; Zhang, Y.; Maric, R.; Yu, H. Pathways to Ultra-Low Platinum Group Metal Catalyst Loading in Proton Exchange Membrane Electrolyzers. *Catalysis Today* **2016**, *262*, 121–132. https://doi.org/10.1016/j.cattod.2015.10.019.

(52) Roller, J. M.; Kim, S.; Kwak, T.; Yu, H.; Maric, R. A Study on the Effect of Selected Process Parameters in a Jet Diffusion Flame for Pt Nanoparticle Formation. *J Mater Sci* **2017**, *52* (16), 9391–9409. https://doi.org/10.1007/s10853-017-1101-y.

(53) Roller, J. M.; Maric, R. A Study on Reactive Spray Deposition Technology Processing Parameters in the Context of Pt Nanoparticle Formation. *J Therm Spray Tech* **2015**, *24* (8), 1529–1541. https://doi.org/10.1007/s11666-015-0322-3.

(54) Roller, J.; Yu, H.; Vukmirovic, M. B.; Bliznakov, S.; Kotula, P. G.; Carter, C. B.; Adzic, R. R.; Maric, R. Flame-Based Synthesis of Core-Shell Structures Using Pd-Ru and Pd Cores. *Electrochimica Acta* **2014**, *138*, 341–352. https://doi.org/10.1016/j.electacta.2014.06.113.

(55) Shiva Kumar, S.; Himabindu, V. Hydrogen Production by PEM Water Electrolysis – A Review. *Materials Science for Energy Technologies* **2019**, *2* (3), 442–454. https://doi.org/10.1016/j.mset.2019.03.002.

(56) Carmo, M.; Fritz, D. L.; Mergel, J.; Stolten, D. A Comprehensive Review on PEM Water Electrolysis. *International Journal of Hydrogen Energy* **2013**, *38* (12), 4901–4934. https://doi.org/10.1016/j.ijhydene.2013.01.151.

(57) Bernt, M.; Hartig-Weiß, A.; Tovini, M. F.; El-Sayed, H. A.; Schramm, C.; Schröter, J.; Gebauer, C.; Gasteiger, H. A. Current Challenges in Catalyst Development for PEM Water Electrolyzers. *Chemie Ingenieur Technik* **2020**, *92* (1–2), 31–39. https://doi.org/10.1002/cite.201900101.

(58) Klose, C.; Trinke, P.; Böhm, T.; Bensmann, B.; Vierrath, S.; Hanke-Rauschenbach, R.; Thiele, S. Membrane Interlayer with Pt Recombination Particles for Reduction of the Anodic

Hydrogen Content in PEM Water Electrolysis. *J. Electrochem. Soc.* **2018**, *165* (16), F1271–F1277. https://doi.org/10.1149/2.1241814jes.

(59) Bessarabov, D. (Invited) Membranes with Recombination Catalyst for Hydrogen Crossover Reduction: Water Electrolysis. *ECS Trans.* **2018**, *85* (11), 17–25. https://doi.org/10.1149/08511.0017ecst.

(60) Price, E. Durability and Degradation Issues in PEM Electrolysis Cells and Its Components. *Johnson Matthey Technology Review* **2017**, *61* (1), 47–51. https://doi.org/10.1595/205651317X693732.

(61) Ouimet, R. Investigation of Highly Stable Proton Exchagne Membrane Water Electrolyzers with Low Catalyst Loading and Reduced Hydrogen Crossover, 2019 Materials Research Society Fall Meeting, Boston, MA, December 3, 2019.

(62) Poozhikunnath, A.; Yu, H.; Bonville, L.; Myles, T.; Maric, R. Characterization and Evaluation of Fe–N–C Electrocatalysts for Oxygen Reduction Directly Synthesized by Reactive Spray Deposition Technology. *J Mater Sci* **2020**, *55* (4), 1673–1691. https://doi.org/10.1007/s10853-019-04124-0.

(63) Rashid, H. U.; Yu, K.; Umar, M. N.; Anjum, M. N.; Khan, K.; Ahmad, N.; Jan, M. T. Catalyst Role in Chemical Vapor Deposition (CVD) Process: A Review. *Rev Adv Mater Sci 40* (3), 235–248.

(64) Zhang, Q.; Sando, D.; Nagarajan, V. Chemical Route Derived Bismuth Ferrite Thin Films and Nanomaterials. *J. Mater. Chem. C* **2016**, *4* (19), 4092–4124. https://doi.org/10.1039/C6TC00243A.

(65) Choy, K. Chemical Vapour Deposition of Coatings. *Progress in Materials Science* **2003**, *48* (2), 57–170. https://doi.org/10.1016/S0079-6425(01)00009-3.

(66) Bryant, W. A. The Fundamentals of Chemical Vapour Deposition. *J Mater Sci* **1977**, *12* (7), 1285–1306. https://doi.org/10.1007/BF00540843.

(67) Spear, K. E. Principles and Applications of Chemical Vapor Deposition (CVD). *Pure and Applied Chemistry* **1982**, *54* (7), 1297–1311. https://doi.org/10.1351/pac198254071297.

(68) Introduction to Chemical Vapour Deposition. In *Chemical Vapour Deposition: An Integrated Engineering Design for Advanced Materials*; Xu, Y., Yan, X.-T., Eds.; Engineering Materials and Processes; Springer: London, 2010; pp 1–28. https://doi.org/10.1007/978-1-84882-894-0_1.

(69) Yan, X.-T.; Xu, Y. *Chemical Vapour Deposition: An Integrated Engineering Design for Advanced Materials*; Engineering Materials and Processes; Springer-Verlag: London, 2010. https://doi.org/10.1007/978-1-84882-894-0.

(70) Tsai, M.-C.; Yeh, T.-K.; Tsai, C.-H. An Improved Electrodeposition Technique for Preparing Platinum and Platinum–Ruthenium Nanoparticles on Carbon Nanotubes Directly Grown on Carbon Cloth for Methanol Oxidation. *Electrochemistry Communications* **2006**, *8* (9), 1445–1452. https://doi.org/10.1016/j.elecom.2006.07.003.

(71) Srinivasan, S.; Velev, O. A.; Parthasarathy, A.; Manko, D. J.; Appleby, A. J. High Energy Efficiency and High Power Density Proton Exchange Membrane Fuel Cells — Electrode Kinetics and Mass Transport. *Journal of Power Sources* **1991**, *36* (3), 299–320. https://doi.org/10.1016/0378-7753(91)87009-Z.

(72) Esteves, L. M.; Oliveira, H. A.; Passos, F. B. Carbon Nanotubes as Catalyst Support in Chemical Vapor Deposition Reaction: A Review. *Journal of Industrial and Engineering Chemistry* **2018**, *65*, 1–12. https://doi.org/10.1016/j.jiec.2018.04.012.

(73) Dupuis, A. The Catalyst in the CCVD of Carbon Nanotubes—a Review. *Progress in Materials Science* **2005**, *50* (8), 929–961. https://doi.org/10.1016/j.pmatsci.2005.04.003.

(74) Danafar, F.; Fakhru'l-Razi, A.; Salleh, M. A. M.; Biak, D. R. A. Fluidized Bed Catalytic Chemical Vapor Deposition Synthesis of Carbon Nanotubes—A Review. *Chemical Engineering Journal* **2009**, *155* (1–2), 37–48. https://doi.org/10.1016/j.cej.2009.07.052.

(75) Guseva Canu, I.; Bateson, T. F.; Bouvard, V.; Debia, M.; Dion, C.; Savolainen, K.; Yu, I.-J. Human Exposure to Carbon-Based Fibrous Nanomaterials: A Review. *International Journal of Hygiene and Environmental Health* **2016**, *219* (2), 166–175. https://doi.org/10.1016/j.ijheh.2015.12.005.

(76) Mukhopadhyay, K.; Koshio, A.; Sugai, T.; Tanaka, N.; Shinohara, H.; Konya, Z.; Nagy, J. B. Bulk Production of Quasi-Aligned Carbon Nanotube Bundles by the Catalytic Chemical Vapour Deposition (CCVD) Method. *Chem Phys Lett* **1999**, *303* (1999), 117–124. https://doi.org/10.1016/S0009-2614(99)00202-X.

(77) Choi, Y. C.; Shin, Y. M.; Lee, Y. H.; Lee, B. S.; Park, G.-S.; Choi, W. B.; Lee, N. S.; Kim, J. M. Controlling the Diameter, Growth Rate, and Density of Vertically Aligned Carbon Nanotubes Synthesized by Microwave Plasma-Enhanced Chemical Vapor Deposition. *Appl. Phys. Lett.* **2000**, *76* (17), 2367–2369. https://doi.org/10.1063/1.126348.

(78) Kanzow, H.; Schmalz, A.; Ding, A. Laser-Assisted Production of Multi-Walled Carbon Nanotubes from Acetylene. *Chem Phys Lett* **1998**, *295* (1998), 525–530. https://doi.org/10.1016/S0009-2614(98)00975-0.

(79) Okazaki, T.; Shinohara, H. Synthesis and Characterization of Single-Wall Carbon Nanotubes by Hot-Filament Assisted Chemical Vapor Deposition. *Chemical Physics Letters* **2003**, *376* (5–6), 606–611. https://doi.org/10.1016/S0009-2614(03)01042-X.

(80) Nikolaev, P.; Bronikowski, M. J.; Bradley, R. K.; Rohmund, F.; Colbert, D. T.; Smith, K. A.; Smalley, R. E. Gas-Phase Catalytic Growth of Single-Walled Carbon Nanotubes from Carbon Monoxide. *Chemical Physics Letters* **1999**, *313* (1–2), 91–97. https://doi.org/10.1016/S0009-2614(99)01029-5.

(81) Sugai, T.; Okazaki, T.; Yoshida, H.; Shinohara, H. Syntheses of Single- and Double-Wall Carbon Nanotubes by the HTPAD and HFCVD Methods. *New J. Phys.* **2004**, *6*, 21–21. https://doi.org/10.1088/1367-2630/6/1/021.

(82) Suekane, O.; Nagasaka, T.; Kiyotaki, K.; Nosaka, T.; Nakayama, Y. Rapid Growth of Vertically Aligned Carbon Nanotubes. *Jpn. J. Appl. Phys.* **2004**, *43* (No. 9A/B), L1214–L1216. https://doi.org/10.1143/JJAP.43.L1214.

(83) Wang, C.; Waje, M.; Wang, X.; Tang, J. M.; Haddon, R. C.; Yan. Proton Exchange Membrane Fuel Cells with Carbon Nanotube Based Electrodes. *Nano Lett.* **2004**, *4* (2), 345–348. https://doi.org/10.1021/nl034952p.

(84) Dai, H.; Rinzler, A. G.; Nikolaev, P.; Thess, A.; Colbert, D. T.; Smalley, R. E. Single-Wall Nanotubes Produced by Metal-Catalyzed Disproportionation of Carbon Monoxide. *Chemical Physics Letters* **1996**, *260* (3–4), 471–475. https://doi.org/10.1016/0009-2614(96)00862-7.

(85) Franklin, N. R.; Li, Y.; Chen, R. J.; Javey, A.; Dai, H. Patterned Growth of Single-Walled Carbon Nanotubes on Full 4-Inch Wafers. *Appl. Phys. Lett.* **2001**, *79* (27), 4571–4573. https://doi.org/10.1063/1.1429294.

(86) Hata, K.; Futaba, D. N.; Mizuno, K.; Namai, T.; Yumura, M.; Iijima, S. Water-Assisted Highly Efficient Synthesis of Impurity-Free Single-Walled Carbon Nanotubes. *Science* **2004**, *306* (5700), 1362–1364. https://doi.org/10.1126/science.1104962.

(87) Bladh, K.; Falk, L. K. L.; Rohmund, F. On the Iron-Catalysed Growth of Single-Walled Carbon Nanotubes and Encapsulated Metal Particles in the Gas Phase. *Applied Physics A: Materials Science & Processing* **2000**, *70* (3), 317–322. https://doi.org/10.1007/s003390050053.

(88) Endo, M.; Kim, Y. A.; Hayashi, T.; Nishimura, K.; Matusita, T.; Miyashita, K.; Dresselhaus, M. S. Vapor-Grown Carbon Fibers (VGCFs) Basic Properties and Their Battery Applications. *Carbon* **2001**, *39* (9), 1287–1297. https://doi.org/10.1016/S0008-6223(00)00295-5.

(89) Shao, Y.; Yin, G.; Zhang, J.; Gao, Y. Comparative Investigation of the Resistance to Electrochemical Oxidation of Carbon Black and Carbon Nanotubes in Aqueous Sulfuric Acid Solution. *Electrochimica Acta* **2006**, *51* (26), 5853–5857. https://doi.org/10.1016/j.electacta.2006.03.021.

(90) Kim, H.; Moon, S. H. Chemical Vapor Deposition of Highly Dispersed Pt Nanoparticles on Multi-Walled Carbon Nanotubes for Use as Fuel-Cell Electrodes. *Carbon* **2011**, *49* (4), 1491–1501. https://doi.org/10.1016/j.carbon.2010.12.020.

(91) Shaijumon, M. M.; Ramaprabhu, S.; Rajalakshmi, N. Platinum/Multiwalled Carbon Nanotubes-Platinum/Carbon Composites as Electrocatalysts for Oxygen Reduction Reaction in Proton Exchange Membrane Fuel Cell. *Appl. Phys. Lett.* **2006**, *88* (25), 253105. https://doi.org/10.1063/1.2214139.

(92) Li, M.; Wu, X.; Zeng, J.; Hou, Z.; Liao, S. Heteroatom Doped Carbon Nanofibers Synthesized by Chemical Vapor Deposition as Platinum Electrocatalyst Supports for Polymer Electrolyte Membrane Fuel Cells. *Electrochimica Acta* **2015**, *182*, 351–360. https://doi.org/10.1016/j.electacta.2015.09.122.

(93) George, S. M. Atomic Layer Deposition: An Overview. *Chem. Rev.* **2010**, *110* (1), 111–131. https://doi.org/10.1021/cr900056b.

(94) O'Neill, B. J.; Jackson, D. H. K.; Lee, J.; Canlas, C.; Stair, P. C.; Marshall, C. L.; Elam, J. W.; Kuech, T. F.; Dumesic, J. A.; Huber, G. W. Catalyst Design with Atomic Layer Deposition. *ACS Catal.* **2015**, *5* (3), 1804–1825. https://doi.org/10.1021/cs501862h.

(95) *Atomic Layer Deposition of Nanostructured Materials*, 1st ed.; Pinna, N., Knez, M., Eds.; Wily-VCH Verlag & Co. KGaA: Weinheim, Germany, 2012.

(96) Johnson, R. W.; Hultqvist, A.; Bent, S. F. A Brief Review of Atomic Layer Deposition: From Fundamentals to Applications. *Materials Today* **2014**, *17* (5), 236–246. https://doi.org/10.1016/j.mattod.2014.04.026.

(97) Mallick, B. C.; Hsieh, C.-T.; Yin, K.-M.; Gandomi, Y. A.; Huang, K.-T. Review—On Atomic Layer Deposition: Current Progress and Future Challenges. *ECS J. Solid State Sci. Technol.* **2019**, *8* (4), N55–N78. https://doi.org/10.1149/2.0201903jss.

(98) Cheng, N.; Shao, Y.; Liu, J.; Sun, X. Electrocatalysts by Atomic Layer Deposition for Fuel Cell Applications. *Nano Energy* **2016**, *29*, 220–242. https://doi.org/10.1016/j.nanoen.2016.01.016.

(99) Setthapun, W.; Williams, W. D.; Kim, S. M.; Feng, H.; Elam, J. W.; Rabuffetti, F. A.; Poeppelmeier, K. R.; Stair, P. C.; Stach, E. A.; Ribeiro, F. H.; Miller, J. T.; Marshall, C. L. Genesis and Evolution of Surface Species during Pt Atomic Layer Deposition on Oxide Supports Characterized by in Situ XAFS Analysis and Water−Gas Shift Reaction. *J. Phys. Chem. C* **2010**, *114* (21), 9758–9771. https://doi.org/10.1021/jp911178m.

(100) Liu, C.; Wang, C.; Kei, C.; Hsueh, Y.; Perng, T. Atomic Layer Deposition of Platinum Nanoparticles on Carbon Nanotubes for Application in Proton-Exchange Membrane Fuel Cells. *Small* **2009**, *5* (13), 1535–1538. https://doi.org/10.1002/smll.200900278.

(101) Shu, T.; Liao, S.-J.; Hsieh, C.-T.; Roy, A. K.; Liu, Y.-Y.; Tzou, D.-Y.; Chen, W.-Y. Fabrication of Platinum Electrocatalysts on Carbon Nanotubes Using Atomic Layer Deposition for Proton Exchange Membrane Fuel Cells. *Electrochimica Acta* **2012**, *75*, 101–107. https://doi.org/10.1016/j.electacta.2012.04.084.

(102) Leus, K.; Dendooven, J.; Tahir, N.; Ramachandran, R.; Meledina, M.; Turner, S.; Van Tendeloo, G.; Goeman, J.; Van der Eycken, J.; Detavernier, C.; Van Der Voort, P. Atomic Layer Deposition of Pt Nanoparticles within the Cages of MIL-101: A Mild and Recyclable Hydrogenation Catalyst. *Nanomaterials* **2016**, *6* (3), 45. https://doi.org/10.3390/nano6030045.

(103) Novak, S.; Lee, B.; Yang, X.; Misra, V. Platinum Nanoparticles Grown by Atomic Layer Deposition for Charge Storage Memory Applications. *J. Electrochem. Soc.* **2010**, *157* (6), H589–H592. https://doi.org/10.1149/1.3365031.

(104) van Ommen, J. R.; Kooijman, D.; Niet, M. de; Talebi, M.; Goulas, A. Continuous Production of Nanostructured Particles Using Spatial Atomic Layer Deposition. *Journal of Vacuum Science & Technology A: Vacuum, Surfaces, and Films* **2015**, *33* (2), 021513. https://doi.org/10.1116/1.4905725.

(105) Celebioglu, A.; Ranjith, K. S.; Eren, H.; Biyikli, N.; Uyar, T. Surface Decoration of Pt Nanoparticles via ALD with TiO2 Protective Layer on Polymeric Nanofibers as Flexible and Reusable Heterogeneous Nanocatalysts. *Sci Rep* **2017**, *7* (1), 13401. https://doi.org/10.1038/s41598-017-13805-2.

(106) Galbiati, S.; Morin, A.; Pauc, N. Supportless Platinum Nanotubes Array by Atomic Layer Deposition as PEM Fuel Cell Electrode. *Electrochimica Acta* **2014**, *125*, 107–116. https://doi.org/10.1016/j.electacta.2014.01.061.

(107) Orak, İ.; Eren, H.; Bıyıklı, N.; Dâna, A. Utilizing Embedded Ultra-Small Pt Nanoparticles as Charge Trapping Layer in Flashristor Memory Cells. *Applied Surface Science* **2019**, *467–468*, 715–722. https://doi.org/10.1016/j.apsusc.2018.10.213.

(108) Xu, S.; Kim, Y.; Park, J.; Higgins, D.; Shen, S.-J.; Schindler, P.; Thian, D.; Provine, J.; Torgersen, J.; Graf, T.; Schladt, T. D.; Orazov, M.; Liu, B. H.; Jaramillo, T. F.; Prinz, F. B. Extending the Limits of Pt/C Catalysts with Passivation-Gas-Incorporated Atomic Layer Deposition. *Nat Catal* **2018**, *1* (8), 624–630. https://doi.org/10.1038/s41929-018-0118-1.

(109) Baker, L.; Cavanagh, A. S.; Yin, J.; George, S. M.; Kongkanand, A.; Wagner, F. T. Growth of Continuous and Ultrathin Platinum Films on Tungsten Adhesion Layers Using Atomic Layer Deposition Techniques. *Appl. Phys. Lett.* **2012**, *101* (11), 111601. https://doi.org/10.1063/1.4749819.

(110) Clancey, J. W.; Cavanagh, A. S.; Kukreja, R. S.; Kongkanand, A.; George, S. M. Atomic Layer Deposition of Ultrathin Platinum Films on Tungsten Atomic Layer Deposition Adhesion Layers: Application to High Surface Area Substrates. *Journal of Vacuum Science & Technology A: Vacuum, Surfaces, and Films* **2015**, *33* (1), 01A130. https://doi.org/10.1116/1.4901459.

(111) Zhang, J.; Chen, C.; Chen, S.; Hu, Q.; Gao, Z.; Li, Y.; Qin, Y. Highly Dispersed Pt Nanoparticles Supported on Carbon Nanotubes Produced by Atomic Layer Deposition for Hydrogen Generation from Hydrolysis of Ammonia Borane. *Catal. Sci. Technol.* **2017**, *7* (2), 322–329. https://doi.org/10.1039/C6CY01960A.

(112) Lee, H.-B.-R.; Bent, S. F. Microstructure-Dependent Nucleation in Atomic Layer Deposition of Pt on TiO_2. *Chem. Mater.* **2012**, *24* (2), 279–286. https://doi.org/10.1021/cm202764b.

(113) Schlicht, S.; Haschke, S.; Mikhailovskii, V.; Manshina, A.; Bachmann, J. Highly Reversible Water Oxidation at Ordered Nanoporous Iridium Electrodes Based on an Original Atomic Layer Deposition. *ChemElectroChem* **2018**, *5* (9), 1259–1264. https://doi.org/10.1002/celc.201800152.

(114) Schlicht, S.; Büttner, P.; Bachmann, J. Highly Active Ir/TiO_2 Electrodes for the Oxygen Evolution Reaction Using Atomic Layer Deposition on Ordered Porous Substrates. *ACS Appl. Energy Mater.* **2019**, *2* (3), 2344–2349. https://doi.org/10.1021/acsaem.9b00402.

(115) Matienzo, D. D.; Settipani, D.; Instuli, E.; Kallio, T. Active IrO2 and NiO Thin Films Prepared by Atomic Layer Deposition for Oxygen Evolution Reaction. *Catalysts* **2020**, *10* (1), 92. https://doi.org/10.3390/catal10010092.

(116) Asundi, A. S.; Raiford, J. A.; Bent, S. F. Opportunities for Atomic Layer Deposition in Emerging Energy Technologies. *ACS Energy Lett.* **2019**, *4* (4), 908–925. https://doi.org/10.1021/acsenergylett.9b00249.

(117) Li, J.; Liang, X.; King, D. M.; Jiang, Y.-B.; Weimer, A. W. Highly Dispersed Pt Nanoparticle Catalyst Prepared by Atomic Layer Deposition. *Applied Catalysis B: Environmental* **2010**, *97* (1–2), 220–226. https://doi.org/10.1016/j.apcatb.2010.04.003.

(118) Brault, P. Plasma Deposition of Catalytic Thin Films: Experiments, Applications, Molecular Modeling. *Surface and Coatings Technology* **2011**, *205* (SUPPL. 2), S15–S23. https://doi.org/10.1016/j.surfcoat.2011.01.052.

(119) Cavarroc, M.; Ennadjaoui, A.; Mougenot, M.; Brault, P.; Escalier, R.; Tessier, Y.; Durand, J.; Roualdès, S.; Sauvage, T.; Coutanceau, C. Performance of Plasma Sputtered Fuel Cell Electrodes with Ultra-Low Pt Loadings. *Electrochemistry Communications* **2009**, *11* (4), 859–861. https://doi.org/10.1016/j.elecom.2009.02.012.

(120) Coutanceau, C.; Brault, P.; Mougenot, M.; Baranton, S.; Ennadjaoui, A.; Cavarroc, M. High Performance Plasma Sputtered Fuel Cell Electrodes with Ultra Low Catalytic Metal Loadings. *ECS Transactions* **2011**, *41* (1), 1151–1159. https://doi.org/10.1149/1.3635648.

(121) Alexeeva, O. K.; Fateev, V. N. Application of the Magnetron Sputtering for Nanostructured Electrocatalysts Synthesis. *International Journal of Hydrogen Energy* **2016**, *41* (5), 3373–3386. https://doi.org/10.1016/j.ijhydene.2015.12.147.

(122) Laurent-Brocq, M.; Job, N.; Eskenazi, D.; Pireaux, J. J. Pt/C Catalyst for PEM Fuel Cells: Control of Pt Nanoparticles Characteristics through a Novel Plasma Deposition Method. *Applied Catalysis B: Environmental* **2014**, *147*, 453–463. https://doi.org/10.1016/j.apcatb.2013.06.021.

(123) Feng, J.; Ramlawi, N.; Biskos, G.; Schmidt-Ott, A. Internally Mixed Nanoparticles from Oscillatory Spark Ablation between Electrodes of Different Materials. *Aerosol Science and Technology* **2018**, *52* (5), 505–514. https://doi.org/10.1080/02786826.2018.1427852.

(124) Lu, J.; Guo, J.; Song, S.; Yu, G.; Liu, H.; Yang, X.; Lu, Z. Preparation of Ag Nanoparticles by Spark Ablation in Gas as Catalysts for Electrocatalytic Hydrogen Production. *RSC Advances* **2020**, *10* (63), 38583–38587. https://doi.org/10.1039/d0ra06682f.

(125) Mauger, S. A.; Neyerlin, K. C.; Yang-Neyerlin, A. C.; More, K. L.; Ulsh, M. Gravure Coating for Roll-to-Roll Manufacturing of Proton-Exchange-Membrane Fuel Cell Catalyst Layers. *Journal of The Electrochemical Society* **2018**, *165* (11), F1012–F1018. https://doi.org/10.1149/2.0091813jes.

TOC Graphic (For Table of Contents Use Only)